J. Fluid Mech. (1976), *vol.* 78, *part* 4, *pp.* 709–736
Printed in Great Britain

On entry-flow effects in bifurcating, blocked or constricted tubes

By F. T. SMITH

Mathematics Department, Imperial College, London

(Received 24 October 1975 and in revised form 10 June 1976)

For practically uniform entry conditions, the features of the steady laminar flow produced by a particular small distortion of the walls of a channel or pipe are shown to alter first from those of the corresponding external situation when the distortion is in an 'adjustment zone', sited a large distance $O(R^{\frac{3}{4}}l)$ from the inlet; $R (\gg 1)$ and l signify respectively a typical Reynolds number and length scale of the incompressible fluid motion. The planar channel flow there develops an extended triple-deck structure, with an unknown inviscid core motion bounded by two-tiered boundary layers near the walls. In three-dimensional pipe flow, where a similar structure occurs, the induced secondary motion has a jet-like nature close to the wall. The size and position of the indentation govern the flow properties within this adjustment regime and both can lead to large-scale effects being propagated. The most substantial effects occur if an indentation, interior blockage or bifurcation is sited just downstream of the adjustment stage in a channel. In a pipe, however, such a siting induces much less upstream influence, and instead the most significant long-scale disturbances are generated when the pipe is constricted asymmetrically over a small length. Vortex motion can then be provoked far beyond the constriction, the sense of rotation changing as the fluid moves further downstream, while upstream source-like secondary flow is found.

1. Introduction

The influence of the entrance conditions on the fluid flow downstream in a pipe (or channel) may be considerable in high Reynolds number motion. For only very far from the inlet can the attached boundary layer emanating from the leading edge of the tube wall be expected to 'fill' the tube, and hence produce fully developed flow even further downstream. So, in any study of high Reynolds number tube flow, the assumption of a fully developed velocity profile implicitly requires the neglect of a vast length of entrance flow and may render the study inapplicable in practice. Again, the entry flow alone can induce some fundamentally important downstream properties, as Singh (1974) and Smith (1976*a*) show for the secondary flow in curved pipes. In seeking to apply theoretical pipe-flow studies to realistic situations there arises a need, therefore, for an investigation of the effects that the entrance conditions may have on the ensuing flow downstream. In particular, for constricted, branching or blocked tubes

there is a need to establish how far from the inlet a particular disturbance, placed at the wall or in the interior, must be before the flow features induced start to alter from the typical undeveloped forms. Beyond that stage, furthermore, what new form does the disturbed flow acquire, given that the oncoming motion is still not necessarily fully developed?

The discussion in this paper is concerned chiefly with the various effects of practically uniform entry conditions on the flow through an indented or branching tube, it being supposed that the fluid is incompressible, that the flow is steady and laminar and that the characteristic Reynolds number R [see (1.1) below] is large. The work is initiated by considering indentations which are compatible with triple-deck theory (Stewartson & Williams 1969; Stewartson 1974; Smith 1973). The position and scale of such an indentation which give rise to the first deviation from wholly undeveloped, quasi-external, characteristics are determined by an order-of-magnitude discussion later in the introduction. There it is shown that, if the length l of the indentation is comparable with the tube width and it is sited in the 'adjustment zone', a distance $O(R^{\frac{3}{8}}l)$ from the inlet, then a new form of interaction takes place between the two viscous wall layers in a channel. This is due to the link which the inviscid core flow establishes between the displacements and pressures in the two layers. The structure of the constricted fluid motion in this primary adjustment zone, set out in §2 for planar channel flows and in §4 for three-dimensional pipe flows, enables the relevance of both the results for quasi-external flow (Smith 1973) and the study of fully developed flow by Smith (1976*b*) to be reviewed by use of linearized analysis. In addition the properties produced by interior blockages and by asymmetric constrictions in pipes prove amenable to analysis. As well as governing the main changeover from wholly undeveloped to fully developed solutions as the indentation *length* is increased, however, the primary adjustment also leads to a discussion of the part played by the *position* of the indentation or blockage. The principal features of two-dimensional and three-dimensional tube flows turn out to be quite distinct then. The former anticipate some of the interaction properties of the asymmetric channel flows described by Smith (1977) when the position is just downstream of the adjustment stage (see §3), whereas the latter introduce a wholly three-dimensional local interaction (see §4). In both cases substantial disturbances can be propagated over lengths much greater than the actual length of the indentation or blockage.

The adjustment length. We derive here, for an indentation in one or both of the otherwise-parallel walls of an infinitely long channel, the critical position and scale which account for the primary changeover from undeveloped to virtually fully developed characteristics in the induced planar motion, before moving on to discuss in §§3 and 4 the allied problems of branching or blockages in a channel and the analogous situations in pipes. It is supposed that the inlet flow is practically uniform (see §2 for a more detailed discussion), its velocity being of magnitude U_0 and directed into the channel. So, sufficiently near the channel entrance, the features of the flow produced in the thin boundary layers and inviscid core by the introduction of small indentations in the channel walls can be analysed in a quasi-external manner, as if the indentations were each placed on a flat plate

in a uniform external stream. There is then effectively no interference between the two plates. Thus the Stewartson triple-deck approach, in particular, would deal with the nonlinear properties of the motion, including the question of separation, if the typical length of indentation were much greater than the thickness of the oncoming boundary layer but much less than the tube width, and provided the indentation height was much less than the boundary-layer thickness, as Smith (1973) has shown. Of more interest, both physically and to the present paper, is the influence of an indentation of length comparable with the tube width. We approach that situation now by considering various positions of the indentation. According to triple-deck theory the uniform stream is disturbed significantly at distances from the wall of the order of the indentation length. Also, if the theory is to remain strictly valid for the different sitings of the indentation, this length must be kept much greater than the boundary-layer thickness. Hence eventually there comes a stage, far downstream, where the individual triple decks around each indentation merge and fill the whole channel. Further downstream we reach a stage where the boundary layers themselves start to coalesce. At even greater distances from the inlet a fully developed state is attained, with the oncoming viscous effects then filling the channel, and the studies by Smith (1976*b*, *c*, 1977) of constrictions of Poiseuille flow become relevant. We contend, however, that the position and scale in the first stage, where the individual triple decks have grown so large that their maximum dimensions are comparable with the channel width, define perhaps the most crucial of the adjustment situations. We seek, therefore, a structure of the motion in which, on reaching the indentation, the boundary layer at each channel wall subdivides essentially into two: an inner zone (the lower deck), of thickness of the order of the indentation height, and an outer zone (the main deck), comprising the majority of the boundary layer. The relatively fast change in displacement thus provoked leads to the setting-up of a potential flow outside, in the upper deck. Since this double structure arises in both boundary layers, the potential flow, being intimately related to both the lower and the main decks, serves to allow an interaction between the flow properties near either indentation.

Suppose this interference takes place when one of the indentations, whose length l is comparable with the channel width lb, is situated a distance $O(l\Delta)$ downstream of the entrance, with the parameter $\Delta\,(\gg 1)$ to be found. Then, since the oncoming boundary layer is still virtually a Blasius one (see §2), its thickness will be in effect $l\delta = l\Delta^{\frac{1}{2}}R^{-\frac{1}{2}}$ and is assumed to be $\ll lb$, which may be justified *a posteriori*. Suppose $l\epsilon\delta$ is the indentation height and $\epsilon\,(\ll 1)$ is unknown. On a length scale $O(l)$ the streamwise velocity $U_0 u$ is then displaced by a relative amount $O(\epsilon)$ in the major part of the boundary layer over the indentation. At distances $O(l\epsilon\delta)$ from the wall, however, a nonlinear viscous interplay is anticipated. Taking $\rho U_0^2\chi$ (ρ being the fluid density and χ an unknown parameter) to be the order of magnitude of the induced pressure, we must have

$$R\epsilon^2 = R\chi = 1/\epsilon\delta^2,$$

from the balance of forces in the Navier–Stokes equations. Here

$$R = U_0 l/\nu \gg 1 \tag{1.1}$$

is the Reynolds number and ν is the kinematic viscosity. Again, the displacement also promotes a small disturbance in the pressure just outside the boundary layer, and a potential flow is induced in the channel core. The small pressure in the core must be of the same order as the relative displacement of the boundary layer. Hence $\chi = \epsilon\delta$ from mass conservation. We may now determine the parameters δ, ϵ, χ and Δ and it is found that

$$\Delta = R^{\frac{3}{8}}, \quad \delta = R^{-\frac{1}{8}}, \quad \epsilon = R^{-\frac{1}{8}}, \quad \chi = R^{-\frac{5}{8}}. \tag{1.2}$$

(These orders also stem from the relation between R and the Reynolds number R_B $(= U_0\bar{x}_0/\nu)$ associated with Blasius flow, since for triple-deck theory to be directly applicable $R = R_B^{\frac{5}{4}}$).

Obviously the same arguments hold for the other indentation. A formal expansion procedure, based on the orders (1.2), can now be set up (§ 2) to examine the changeover occurring when the indentations are placed at distances $O(R^{\frac{3}{8}}l)$ from the channel entrance. In fact the scalings (1.2) apply equally well to the primary adjustment in pipe flows, discussed in § 4. In both pipes and channels some care must be taken to correct the oncoming Blasius boundary layer and inviscid core for the secondary effects due to the Blasius displacement, especially since the boundary layer is growing indefinitely downstream, and this aspect is also considered in §§ 2 and 4. Linearized solutions of the governing equations at adjustment are presented in §§ 3 and 4 both for the flow through constricted or dilated tubes and for the features induced by a blockage in a pipe or channel or bifurcation in a channel.

We non-dimensionalize the problem at this stage, letting $(u, v)\,U_0$ be the velocities in the $(\bar{x}, y)$ directions respectively, where $l\bar{x}$ and ly measure distances along and across the channel with origin at the leading edge of the lower plate. The pressure is written as $\rho U_0^2(p + p_0)$, where $\rho U_0^2 p_0$ is the inlet value.

2. The adjustment in channels

For convenience we take

$$\epsilon = R^{-\frac{1}{8}} \ll 1 \tag{2.1}$$

to be the fundamental parameter in our expansions of the solution near the indentations. The indentations therefore have their starting points at a distance $\epsilon^{-3}l\bar{x}_0 + O(l)$, say, downstream of the entrance, where $\bar{x}_0 \sim 1$, and we set $\bar{x} = \epsilon^{-3}\bar{x}_0 + x$, where $x = O(1)$. The walls have the shapes

$$y = \begin{cases} \epsilon^2 hF(x) & \text{(lower indentation),} \\ b - \epsilon^2 hG(x) & \text{(upper indentation).} \end{cases} \tag{2.2}$$

Here the constant $h \sim 1$ and $F(-\infty) = G(-\infty) = 0$.

Our attention will be focused initially on the flow properties concerned with the lower indentation, since those for the upper wall follow by the same reasoning. The solution for the oncoming Blasius boundary layer and its lower-order contributions has been discussed by Wilson (1971) and Van Dyke (1970) and now needs some consideration. The nature of the core and the expanding boundary layers, which constitute the initial distribution for our indentation study, depends

vitally on the prescribed inlet conditions at $\bar{x} = 0$, but only for finite distances from the inlet: far downstream the differences between the various entry flows considered by Van Dyke (1970) and Wilson (1971) decay relatively fast. If these conditions specify a uniform entry flow, then the solution for the lower boundary layer, in which $y = R^{-\frac{1}{2}}\bar{Y}$ and $\bar{Y}$ is $O(1)$, develops according to

$$u \approx f'_B(\eta) + \sum_{n=2}^{\infty} f'_n(\eta)\,(\bar{x}R)^{\tau_n - \frac{1}{2}}\,2^{-\frac{1}{2}} + \left(\frac{\bar{x}}{R}\right)^{\frac{1}{2}} f'_{B1}(\eta), \quad \eta = \bar{Y}/(2\bar{x})^{\frac{1}{2}}, \tag{2.3a}$$

for $\bar{x}$ large but $\ll R$, and similarly in the core for $0 < y < b$. Here $\tau_n = 2^{-n}$ for $n \geqslant 2$ and $f'_B(\eta)$ is the Blasius velocity, given by

$$f'''_B + f_B f''_B = 0, \quad f_B(0) = f'_B(0) = 0, \quad f'_B(\infty) = 1 \tag{2.3b}$$

and with the properties

$$f_B \sim \frac{\lambda_B}{2}\eta^2 - \frac{\lambda_B^2 \eta^5}{5!} + \ldots \quad \text{for} \quad \eta \ll 1, \quad \lim_{\eta\to\infty}(\eta - f_B) = \beta_B = 1.21678\ldots, \tag{2.3c}$$

where $\lambda_B = 0{\cdot}46960\ldots$. The functions $f_n(\eta)$ satisfy linear homogeneous equations with no-slip boundary conditions and $f_n \sim A_n \eta^{2\tau_n} + B_n$ as $\eta \to \infty$. Here A_n and B_n are constants (calculated by Wilson (1971) for $2 \leqslant n \leqslant 7$). Also, $f_{B1}(\eta)$ is a readily calculable function with

$$f_{B1}(0) = f'_{B1}(0) = 0, \quad f'_{B1}(\infty) = \beta_B \sqrt{2}.$$

The solution (2.3a) in fact becomes invalid when $\bar{x} \sim R \gg 1$ (as well as in a small leading-edge zone where $\bar{x}$ is $O(R^{-1})$). This anticipates the merging of the two boundary layers which emanate from $(\bar{x}, y) = (0, 0)$ and $(\bar{x}, y) = (0, b)$ and the setting up of a boundary-layer-type problem across the entire channel when $\bar{x}$ is $O(R)$. The terms in $\bar{x}/R$ in (2.3a) then follow from analysis of the flow when $\bar{x}/R$ takes a small, $O(1)$ value. Our present position of the indentation is not as far downstream as this, but the terms in (2.3a) still need some consideration. When x is $O(1)$ the boundary layer is described by

$$\left.\begin{aligned} u &= U_B(Y) + \epsilon U_{B1}(Y) + \sum_{n=2}^{\infty} \epsilon^{4-8\tau_n} U^{(n)}(Y) + O(\epsilon^2); \\ U_B(Y) &= f'_B(\eta), \quad U^{(n)}(Y) = 2^{-\frac{1}{2}} f'_n(\eta)\,\bar{x}_0^{\tau_n - \frac{1}{2}}, \quad U_{B1}(Y) = \bar{x}_0^{\frac{1}{2}} f'_{B1}(\eta). \end{aligned}\right\} \tag{2.4}$$

Similar expressions hold for the pressure and transverse velocity, and

$$Y = \epsilon^{-1} y = (2\bar{x}_0)^{\frac{1}{2}}\eta \sim 1$$

implies that the variation with respect to x is of relative order ϵ^3. An analogous result holds for the less artificial inlet conditions studied by Van Dyke and Wilson, those for an infinite cascade and for an irrotational entry flow, except that the terms $U^{(n)}(Y)$ in (2.4) are then absent. Hence, whatever the initial conditions, in effect we are considering below the extra velocities and pressures induced by the indentations alone. Then (2.4) constitutes the solution for x large and negative, while v and p are found to be $O(\epsilon^4)$ and $O(\epsilon)$ respectively as $\bar{x} \uparrow \epsilon^{-3}\bar{x}_0$.

In the main part of the boundary layer over the lower indentation, the main

deck, where $Y \sim 1$, the solution consistent with the results of §1 and (2.1)–(2.4) has the expansion (cf. Stewartson 1974)

$$\left.\begin{aligned} u &= U_B(Y) + \epsilon[A(x)\,U_B'(Y) + U_{B1}(Y)] + O(\epsilon^2), \\ v &= -\epsilon^2 A'(x)\,U_B(Y) + O(\epsilon^3), \quad p = \epsilon p_{1B} + \epsilon^2[p_1(x, Y) + p_{2B}] + O(\epsilon^3) \end{aligned}\right\} \tag{2.5}$$

when $x \sim 1$. Here $p_{1B} = -\beta_B(2\bar{x}_0)^{\frac{1}{2}}$ and p_{2B} are constants associated with the oncoming boundary layer. The function $A(x)$ is unknown but satisfies $A(-\infty) = 0$ from (2.4). The y-momentum equation gives the result $\partial p_1/\partial Y = 0$, so that $p_1 = P(x)$, say, where $P(x)$ is a function of x to be determined. Lower-order terms in (2.5) are also obtainable. The displacement in (2.5), assumed non-zero, induces a slip velocity at $Y = 0$, however, and a thin viscous zone, the lower deck, is thereby generated. If $y = \epsilon^2 Z$ then, since $U_{B1}(0) = U^{(n)}(0) = 0$, the velocities and pressure for $Z \sim 1$ acquire the forms $u = \epsilon U(x, Z)$, $v = \epsilon^3 V(x, Z)$ and $p = \epsilon p_{1B} + \epsilon^2(P(x) + p_{2B})$ to leading order. Here the result $\partial p/\partial Z = 0$ from the transverse momentum equation has been anticipated, and the ϵ^2 term in u vanishes as $x \to -\infty$. To first order in ϵ the governing equations in this lower zone are the boundary-layer equations

$$\frac{\partial U}{\partial x} + \frac{\partial V}{\partial Z} = 0, \quad U\frac{\partial U}{\partial x} + V\frac{\partial U}{\partial Z} = -P'(x) + \frac{\partial^2 U}{\partial Z^2} \tag{2.6a}$$

subject to the boundary conditions

$$\left.\begin{aligned} &U = V = 0 \quad \text{on} \quad Z = hF(x), \\ &U \sim \lambda_B(2\bar{x}_0)^{-\frac{1}{2}}(Z + A(x)) \quad \text{as} \quad Z \to \infty, \\ &U \sim \lambda_B(2\bar{x}_0)^{-\frac{1}{2}} Z \quad \text{as} \quad x \to -\infty. \end{aligned}\right\} \tag{2.6b}$$

The conditions (2.6*b*) allow for no slip at the indentation (2.2), for the merging with the main deck (2.5) as $Y \to 0$ and for continuation with the oncoming boundary layer (2.3) with (2.4), in turn. To fix the problem for the evaluation of $P(x)$ and $A(x)$, the flow outside the boundary layer, where $y \sim 1$, and also the features near the upper wall, must be examined as well. Since $v_1 \sim -A'(x)$, $p_1 = P(x)$ and $u_1 \to 0$ as $Y \to \infty$, the motion in the core outside the boundary layer is given by

$$u = 1 + \epsilon\hat{U}_1(y, \epsilon) + \epsilon^2 U_2(x, y), \quad v = \epsilon^2 V_2(x, y), \quad p = \epsilon p_{1B} + \epsilon^2[P_2(x, y) + p_{2B}] \tag{2.7}$$

for $x \sim 1$. The function $\hat{U}_1(y, \epsilon)$, of order one generally, denotes the perturbations to the uniform stream $u = 1$ in the inviscid core far ahead of the indentation [see Wilson 1971, equations (3.30)–(3.32)]. From the Navier–Stokes equations it is found that this region is essentially one of potential flow and that V_2 satisfies Laplace's equation

$$\partial^2 V_2/\partial x^2 + \partial^2 V_2/\partial y^2 = 0 \tag{2.8a}$$

for $-\infty < x < \infty$, $0 < y < b$. The boundary conditions on V_2 at $y = 0$ are implied by matching with the solution in the main deck as $Y \to \infty$. Use of the relation $\partial V_2/\partial y = \partial P_2/\partial x$ therefore gives

$$V_2(x, 0) = -A'(x), \quad \partial V_2(x, 0)/\partial y = P'(x). \tag{2.8b}$$

The constraints on V_2 at $y = b$ are completely analogous to (2.8*b*). For, as in (2.5) and (2.6) near the upper wall the flow splits up into two zones, one where

$(b-y)\epsilon^{-1} = \tilde{Y}$ is $O(1)$ and the thinner lower deck, where $(b-y)\epsilon^{-2} = \tilde{Z}$ is $O(1)$. The crucial problem is then essentially identical with (2.6) except for an unknown pressure term $\tilde{P}(x)$ and displacement $\tilde{A}(x)$, say, instead of P and A, and the no-slip condition is required at $\tilde{Z} = hG(x)$. Hence we may impose on the potential flow in the core the constraints

$$V_2(x,b) = \tilde{A}'(x), \quad \partial V_2(x,b)/\partial y = \tilde{P}'(x). \tag{2.8c}$$

Thus the flow through the constricted channel is controlled by the solution (2.8*a–c*) to the inviscid core, together with the solutions to the lower and upper viscous sublayers, characterized by (2.6*a*, *b*) and its counterpart for $\tilde{Z} \sim 1$. The elliptic nature of the governing equation in the core means that not only is upstream influence introduced but also the two viscous sublayer flows are intimately related, via the four unknown functions $A(x)$, $P(x)$, $\tilde{A}(x)$ and $\tilde{P}(x)$.

The core flow (2.8*a–c*) may now be solved formally by applying the Fourier transform with respect to x:

$$V_2^*(\omega, y) = \int_{-\infty}^{\infty} e^{-i\omega x} V_2(x,y)\, dx, \tag{2.9}$$

where ω is the complex transform variable. This gives, from (2.8*a*), the result that V_2^* is a linear combination of the functions $\exp(\pm\omega y)$ with coefficients dependent on ω alone. Application of the boundary conditions (2.8*b*, *c*) then yields the expressions for the transforms of the pressure gradients $Q(x) = P'(x)$ and $\tilde{Q}(x) = \tilde{P}'(x)$ in terms of the displacements $A(x)$ and $\tilde{A}(x)$:

$$Q^*(\omega) = i\omega^2[A^*(\omega)\coth\omega b + \tilde{A}^*(\omega)\operatorname{cosech}\omega b], \tag{2.10a}$$

$$\tilde{Q}^*(\omega) = i\omega^2[A^*(\omega)\operatorname{cosech}\omega b + \tilde{A}^*(\omega)\coth\omega b]. \tag{2.10b}$$

The superscript * denotes functions transformed as in (2.9).

The pressure–displacement laws (2.10*a*, *b*) clearly simplify if x is large or small (ω small or large respectively), or if b takes an extreme value. The nature of these simplifications, and of the dependence on $\bar{x}_0$ of the solution to (2.6), is perhaps more readily seen from the linearized theory presented below.

3. Wall indentations, blockages and bifurcations: linearized solutions in channels

3.1. *Wall indentations*

If there are indentations at the walls, as supposed in §2, then for general values of h in (2.2) the crucial problem of the interactions between the inviscid core flow and the double-structured boundary layers along the channel walls requires a numerical approach to the viscous equations (2.6*a*, *b*) and their counterparts for $\tilde{Z} \sim 1$, along with the pressure–displacement laws (2.10*a*, *b*), and the motion is nonlinear. Here we shall confine our observations on constricted channel flows to the properties for small values of h, to derive the basic influence of the walls on the motion, and obtain linearized solutions.

When $h \ll 1$ the lower-wall solution is expressible in the form

$$U = \mu Z + h\bar{U}, \quad P'(x) = h\bar{Q}(x), \quad V = h\bar{V}, \quad A(x) = h\bar{A}(x),$$

where the parameter $\mu = (2\bar{x}_0)^{-\frac{1}{2}}\lambda_B$ is $O(1)$. Substitution into the governing equations (2.6a, b) and neglecting terms of order h^2 eventually yields for the transformed variables the relation

$$-\bar{Q}^*(\omega) = \mu^{\frac{1}{3}}\theta^{\frac{4}{3}}(0+i\omega)^{\frac{2}{3}}[F^*(\omega)+\bar{A}^*(\omega)], \tag{3.1}$$

from Smith (1973). Here $\theta = [-3\,\mathrm{Ai}'(0)]^{\frac{1}{3}} = 0{\cdot}8272\ldots$, Ai is the Airy function, the function $(0 \pm i\omega)^n$ has a branch cut extending from $\pm 0i$ to $\pm\infty i$ in the ω plane and its argument lies between $-n\pi$ and $n\pi$. Analogous expansions and solutions in the upper wall layer produce the requirement

$$-\bar{\tilde{Q}}^*(\omega) = \mu^{\frac{1}{3}}\theta^{\frac{4}{3}}(0+i\omega)^{\frac{2}{3}}[G^*(\omega)+\bar{\tilde{A}}^*(\omega)]. \tag{3.2}$$

Hence, with (2.10a, b) (where Q, $\tilde{Q}$, A and $\tilde{A}$ can be replaced by $\bar{Q}$, $\bar{\tilde{Q}}$, $\bar{A}$ and $\bar{\tilde{A}}$), we have sufficient equations to fix the solution. It follows that when b and μ are $O(1)$ the linear equations

$$\left.\begin{aligned}(\bar{A}^*+\bar{\tilde{A}}^*)[i\omega^2\coth(\tfrac{1}{2}\omega b)+(0+i\omega)^{\frac{2}{3}}\theta^{\frac{4}{3}}\mu^{\frac{1}{3}}] &= -(F^*+G^*)(0+i\omega)^{\frac{2}{3}}\theta^{\frac{4}{3}}\mu^{\frac{1}{3}},\\ (\bar{A}^*-\bar{\tilde{A}}^*)[i\omega^2\tanh(\tfrac{1}{2}\omega b)+(0+i\omega)^{\frac{2}{3}}\theta^{\frac{4}{3}}\mu^{\frac{1}{3}}] &= -(F^*-G^*)(0+i\omega)^{\frac{2}{3}}\theta^{\frac{4}{3}}\mu^{\frac{1}{3}}.\end{aligned}\right\} \tag{3.3}$$

fix the two inviscid displacements and hence the pressure gradients from (3.1) and (3.2). Inversion of the transforms is difficult in general but simplifies when b or μ takes an extremely small or large value.

Indeed, if $b \gg 1$ the pressure–displacement laws (2.10a, b) possess more recognizable forms no matter what the value of h, since then

$$Q^* = i\omega\,|\omega|\,A^*, \quad \tilde{Q}^* = i\omega\,|\omega|\,\tilde{A}^*,$$

$$\text{or} \qquad A''(x) = \frac{-1}{\pi}\int_{-\infty}^{\infty}\frac{P'(\xi)\,d\xi}{x-\xi} \quad \tilde{A}''(x) = \frac{-1}{\pi}\int_{-\infty}^{\infty}\frac{\tilde{P}'(\xi)\,d\xi}{x-\xi} \tag{3.4}$$

(provided that $|\omega| \gg b^{-1}$, i.e. $|x| \ll b$). Thus, when the walls are far enough apart, i.e. when the channel width greatly exceeds the indentation length, the features of the upper- and lower-wall flow become quite unrelated and are quasi-external phenomena, since (3.4) are the results of thin-wing theory. For each the study by Smith (1973) is pertinent. In particular the solutions (3.3) are now those given by Smith's linearized treatment and substantial upstream influence is inherent in the motion. When $b \ll 1$ on the other hand, we find that to first order the pressure in the channel core remains constant at any downstream station. From (2.10a, b) and (3.3), even in the nonlinear case, $P = \tilde{P}\,[= A_1 + \tilde{A}_1]$ if $A = A_0 + bA_1$ and $\tilde{A} = \tilde{A}_0 + b\tilde{A}_1$ to $O(b)$. Also

$$A_0(x) = -\tilde{A}_0(x) = \tfrac{1}{2}[G(x)-F(x)] \tag{3.5}$$

provided that $F(x)+G(x)$ remains order one. Effectively, then, the core suffers a completely uniform cross-displacement equal to the average of the wall displacements. This property links the solution to that of Smith (1976b), who solved the fully developed situation for $h \sim 1$, when (3.5) holds exactly. When the total distortion $F+G$ is $O(b^{-1})$ as well but the difference $F-G$ remains $O(1)$, the result (3.5) is modified slightly. Nevertheless we may conclude that the

confinement of the motion by the walls when they are relatively close together almost entirely suppresses the upstream influence and that the viscous effects already dominate practically the whole tube flow. A comparison between the solutions for an indentation at the lower wall when $b \ll 1$ and those for $b \gg 1$ may be made by referring to figures 5 and 7 of Smith (1976*b*) and to figure 3 of Smith (1973) respectively. Clearly the nature of the constricted flow field, and especially the upstream influence, if any, is crucially dependent upon the typical *length* of indentation compared with the channel width.

We consider next, therefore, the part played by the *positioning* of the indentations relative to the $O(R^{\frac{3}{7}}l)$ adjustment distance. Suppose that the indentations are placed just upstream of the primary adjustment position, i.e. $\bar{x}_0 \ll 1$ or $\mu \gg 1$. Then (3.3) indicates that to first order $A = -F$ and $\tilde{A} = -G$. The double wall layers are consequently of little importance. The fluid there suffers a complete displacement parallel to the indentations, and from (2.10) the core behaves as if it were simply an inviscid flow within the given channel. In particular, if b is now taken to be large as well, this core flow is virtually unaffected by the constriction except close to each of the walls, where it assumes the form of the classical, thin-wing, inviscid motion past a prescribed surface. When b is small, however, the pressure again stays constant across the core, owing to the thinning of the channel, and is given by $P = \tilde{P} = -(F+G)/b$. The similarity between this result and that in (3.5) and above arises from the smallness of b. However, here the inviscid core dominates the flow and the viscous effects are negligible, whereas in (3.5) the opposite is true. When $\mu \gg 1$ the oncoming Blasius flow is more attached to the wall and so the viscous forces have little effect on it, leaving the inviscid behaviour. Conversely, when $b \ll 1$ but μ is finite the core's influence is diminished, simply because the streamwise length scale is much greater than the channel width. So then the flow becomes effectively fully developed.

Of more interest are the flow features when the indentations are just downstream of the adjustment, i.e. when $\mu \ll 1$, but with $b \sim 1$, so that the constriction length remains comparable with the tube width. Here it is found that the fluid first responds considerably at a distance upstream much greater than the actual length of constriction, while downstream the wake effect persists over an even larger distance. We shall concern ourselves below only with these long-scale features and omit the details of the motion nearer the indentations. In the motion far downstream or upstream of the constriction the major contributions to the solution stem from the behaviour of the transforms for $|\omega|$ small. Inspection of (3.3) therefore suggests two principal zones of interest when μ is small, namely $|\omega| \sim \mu^5$ and $|\omega| \sim \mu^{\frac{5}{7}}$. The first propagates the most persistent effect in the wake but is found to have no upstream significance [see (3.7) below], and it is the second zone that is responsible for the upstream influence. The contributions from $O(1)$ values of $|\omega|$ are exponentially small when $|x|$ takes any large value, according to (3.3). Setting $\omega = \mu^5\Omega_1$ in (3.3) we obtain, for Ω_1 of order one,

$$\left.\begin{aligned} \bar{A}^* &= \tfrac{1}{2}[G^*(0) - F^*(0)] - \frac{b(0+i\Omega_1)^{\frac{3}{5}}\theta^{\frac{4}{5}}[F^*(0)+G^*(0)]}{2[2i\Omega_1 + b(0+i\Omega_1)^{\frac{3}{5}}\theta^{\frac{4}{5}}]}, \\ \bar{\tilde{A}}^* &= \bar{A}^* - G^*(0) + F^*(0), \end{aligned}\right\} \tag{3.6}$$

so that $\bar{A}^*$ is regular throughout the lower half of the Ω_1 plane. The constants $F^*(0)$ and $G^*(0)$ are effectively the cross-sectional areas of the indentations. Inversion of the transform then yields, for a distortion of the lower wall only ($G = 0$), for example,

$$\bar{A}(x) = \begin{cases} -F^*(0)\dfrac{\mu^5 3^{\frac{1}{2}}\theta^4 b^3}{32\pi}\mathscr{H}_1 \quad \left(\mathscr{H}_n(X_1) = \displaystyle\int_0^\infty \frac{\xi^{\frac{1}{3}n}\exp\left(-\frac{1}{8}\xi X_1\theta^4 b^3\right)d\xi}{1+\xi^{\frac{1}{3}}+\xi^{\frac{2}{3}}}\right) \\ \qquad\qquad\qquad\qquad\qquad\qquad\qquad \text{for} \quad X_1 > 0, \\ 0 \quad \text{for} \quad X_1 < 0, \end{cases} \tag{3.7}$$

where $x = \mu^{-5}X_1 \gg 1$. Similarly we find

$$(\tau - \mu,\ P'(x)) = \frac{hF^*(0)}{128\pi}\, 3^{\frac{1}{2}}\theta^{\frac{16}{3}}\mu^8 b^4(-6\mathrm{Ai}\,(0)(\mathscr{H}_2 + \mathscr{H}_3), b\mu^2\theta^{\frac{8}{3}}\mathscr{H}_4) \tag{3.8}$$

for $X_1 > 0$. Here τ is the scaled skin friction $(\partial U/\partial Z)_{z=0}$. Upstream $\tau = \mu$ and $P'(x) = 0$ when $X_1 \sim 1$, and no effect is felt. Instead the upstream influence comes from setting $\omega = \mu^{\frac{5}{7}}\Omega_2$ in (3.3), with $\Omega_2 \sim 1$. This produces to first order

$$\bar{A}^* = [G^*(0) - F^*(0)]\,(0 + i\Omega_2)^{\frac{2}{3}}\theta^{\frac{4}{3}}/[ib\Omega_2^3 + 2(0 + i\Omega_2)^{\frac{2}{3}}\theta^{\frac{4}{3}}], \tag{3.9}$$

and leaves $\bar{A}^*(\omega)$ with a pole in the lower half-plane at $\Omega_2 = -i\kappa$, where $\kappa = (2^3\theta^4 b^{-3})^{\frac{1}{7}}$. We are interested in this solution for negative values of $\mu^{\frac{5}{7}}x$ alone, since (3.7) and (3.8) give the dominant terms for x large and positive. Inversion of (3.9) supplies the main contribution to the upstream solution:

$$\bar{A}(x) = (-3/7b)\,F^*(0)\,(\tfrac{1}{2}b\theta)^{\frac{4}{7}}\mu^{\frac{5}{7}}\exp(\kappa X_2) \quad \text{for} \quad X_2 < 0 \tag{3.10}$$

for the constriction with $G = 0$, where $x = \mu^{-\frac{5}{7}}X_2 \gg 1$. Other physically interesting results for x large and negative may be worked out similarly; e.g.

$$(\tau - \mu, P'(x)) = (3h/7b)\,F^*(0)\,\mu^{\frac{15}{7}}\theta^{\frac{16}{21}}(\tfrac{1}{2}b)^{\frac{2}{7}}(-3\,\mathrm{Ai}\,(0)\,(\tfrac{1}{2}b)^{\frac{1}{7}}, \mu^{\frac{4}{7}}\theta^{\frac{32}{21}})\exp(\kappa X_2). \tag{3.11}$$

Graphs of these predominant upstream and downstream solutions are presented in figure 1. Because of the long length scales involved both ahead and in the wake, the constriction acts merely as a point disturbance and, interestingly enough, the flow behaves in a manner not unlike that for a point disturbance in external flow (e.g. Smith 1973, figure 4). Thus the displacement $A(x)$, pressure gradient $P'(x)$ and skin-friction perturbation $\tau(x) - \mu$ are singular as $X_1 \to 0+$ and proportional to $X_1^{-\frac{2}{3}}$, $X_1^{-\frac{5}{3}}$ and $X_1^{-\frac{4}{3}}$ respectively. Upstream the rising pressure causes an upward displacement in the main boundary layer and the skin friction falls. Far downstream the displacement is again upward and the skin friction returns to the value far upstream from below under the favourable pressure gradient. The basic physical reasons for the generation of such long-scale interactions here must be quite different from those in external flow, however, since the walls are comparatively close together when viewed from points where $|x| \sim \mu^{-5}$ or $\mu^{-\frac{5}{7}}$. The upstream interactions for $\mu \ll 1$ are apparently due instead to the actions of a small pressure gradient *across* the channel, within the inviscid core. Indeed, even though the indentations here are considered to be moved only just downstream of the primary adjustment zone, this link between the wall

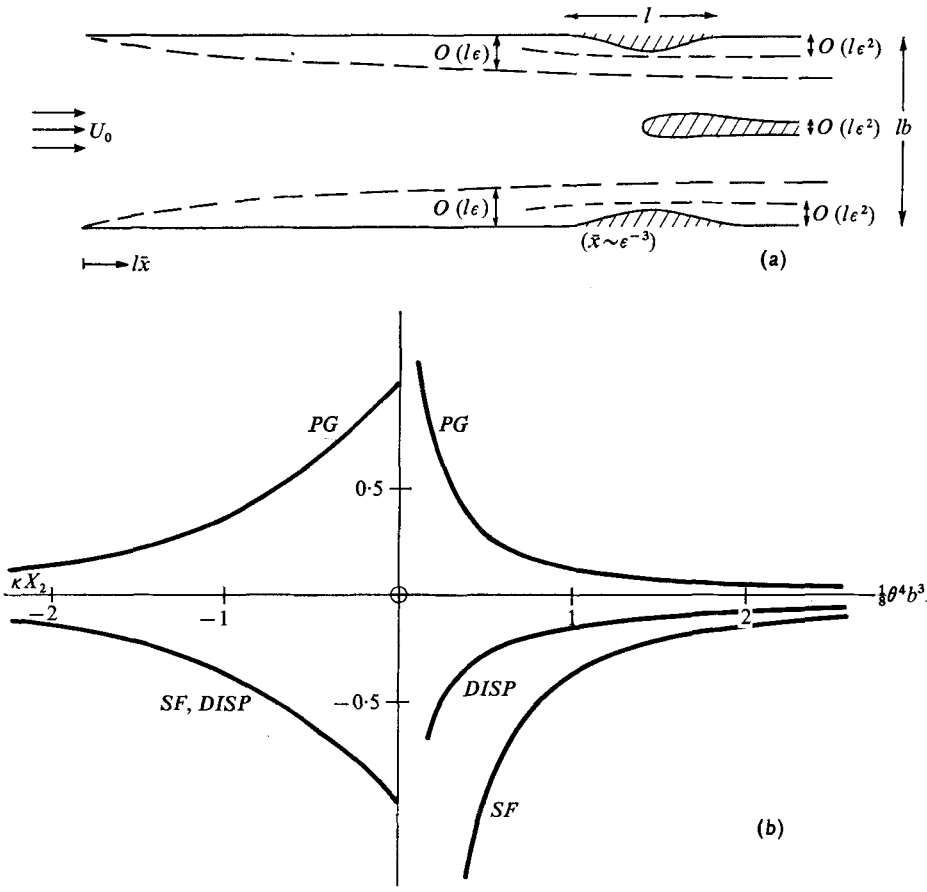

FIGURE 1. (*a*) Schematic diagram of the core and double boundary-layer structure for an indented and bifurcating channel at the adjustment stage. (*b*) The long-scale upstream and downstream linearized solutions in a constricted channel when $\mu \ll 1$. Here, for $X_2 < 0$, $PG = 7b(2/b)^{\frac{2}{7}}\bar{P}'(x)/3\mu^{\frac{2}{7}}\theta^{\frac{1}{7}}F^*(0)$, $SF = 7b\kappa(\tau-\mu)/9h\,\mathrm{Ai}\,(0)\,\mu^{\frac{1}{7}}\theta^{\frac{4}{3}}F^*(0)$, $DISP = 7b(2/b\theta)^{\frac{4}{7}} \times \bar{A}(x)/3\mu^{\frac{5}{7}}F^*(0)$, while for $X_1 > 0$, $PG = 128\pi\bar{P}'(x)/3^{\frac{1}{2}}\mu^{10}\theta^8b^5F^*(0)$, $SF = 64\pi(\tau-\mu)/3^{\frac{3}{2}}h\,\mathrm{Ai}\,(0)\,\mu^8\theta^{\frac{16}{3}}b^4F^*(0)$, $DISP = 32\pi\bar{A}(x)/3^{\frac{1}{2}}\mu^5\theta^4b^3F^*(0)$.

layers, maintained via the core, is surprisingly reminiscent of the large-scale upstream response that takes place within an asymmetric channel when the oncoming flow is fully developed, which is described by Smith (1977). In either situation the shear stress at one wall ($y = 0$, say) falls owing to the increase in pressure there, and so the boundary layer expands. Because in the present problem the uniform stream has a diminished effect compared with the now much thicker and less attached Blasius flow, the core suffers a complete displacement towards the opposite wall ($y = b$). The flow across the channel associated with this displacement then sets up the pressure difference between the two walls, and the pressure at $y = b$ becomes negative. This pressure drop therefore sustains the increase in shear stress at $y = b$ and the fall in displacement there is accentuated. Hence the exponential type of upstream behaviour develops. In contrast, the behaviour far downstream is dictated by the boundary layer and the core

plays little part, again because of the increased influence of the Blasius layer. The boundary layer, having encountered the indentation, returns to its original Blasius state and both the displacement and pressure therefore fall. The pressure is effectively constant across the channel (the solution being essentially that for $b \ll 1$), as the wake disturbances are sustained over distances much greater than those defining the upstream influence. Hence the displacement of each boundary layer must be the same relative to the adjoining wall. The pressure itself is then directly proportional to the average boundary-layer displacement.

Many aspects of injection and other wall conditions can be treated in a similar manner, but we turn now to a discussion of the influence of a disturbance placed in the interior of the tube.

3.2. *Bifurcations or blockages*

If a body, whether of finite length (as with a blockage, measuring instrument or model of a wing section) or semi-infinite (as with a simple branching of the tube), is fixed in the interior of the channel, its effects on the flow field may be analysed by our present methods if we suppose that its starting point is situated a distance $O(R^{\frac{3}{8}}l)$ from the inlet and that its thickness is typically a fraction $O(R^{-\frac{2}{5}})$ of the channel width lb. For then the perturbations produced in the potential core flow may be assumed to be of relative order ϵ^2, consistent with the core structure. Also, the boundary layer induced on the body surface can be expected to have thickness $\sim R^{-\frac{1}{2}}l = \epsilon^{\frac{1}{2}}l$ when $|x|$ is finite and so can be neglected to first order, provided it does not separate. A thicker body would presumably cause a gross change in the character of the whole channel flow (cf. Smith 1977) and a thinner one distorts the oncoming flow by a negligibly small amount. For definiteness we shall usually suppose the body to be semi-infinite and discuss mainly the bifurcation aspect.

The broad structure of the solution at adjustment is unaltered in its essentials. Thus near either wall the oncoming boundary layer gradually evolves a two-tiered form as the bifurcation is approached. The lower wall layer is governed by (2.6a, b) but with $F(x) = 0$ if the channel remains straight, and similarly for the upper layer with $G(x)$ assumed to be zero. The thick dividing body in the inviscid core excites these two double-structured interactions by provoking $O(\epsilon^2)$ pressure and displacement distributions at the edges $y = 0+$, $b-$ of the two boundary layers. If the body is centred a distance lc ($0 < c < b$) from the lower wall, we suppose it to be described by

$$y = \begin{Bmatrix} c + \epsilon^2 hS(x) & \text{(upper surface)} \\ c - \epsilon^2 hT(x) & \text{(lower surface)} \end{Bmatrix} \tag{3.12}$$

for $x \geqslant 0$, with $S(0) = T(0) = 0$ and $h \sim 1$. The core flow is therefore given by the expansion (2.7) to order ϵ^2, and so by the solution of the Laplace equation (2.8a) for V_2. Conditions (2.8b, c) hold at $y = 0, b$, and in $x > 0$

$$V_2(x, c+) = hS'(x), \quad V_2(x, c-) = -hT'(x). \tag{3.13}$$

Here (3.13) is the constraint for tangential flow at the body surface, the full no-slip condition being relaxed and implying the existence of the $O(\epsilon^{\frac{1}{2}}l)$ boundary layer adjoining the surface (3.12).

For a semi-infinite body or bifurcation the solution for $V_2(x, y)$ may be obtained in principle by applying the Fourier transform (2.9) and using a Wiener–Hopf technique (Jones 1952; Noble 1958). The transformed Laplace equation with the boundary conditions (2.8*b*, *c*) at the walls gives V_2^* in terms of the pressures and displacements. At $y = c$ the function $V_2(x, y)$ is discontinuous in $x > 0$ but, together with its first derivative, is assumed continuous for $x < 0$. Accordingly we find, on applying (3.13),

$$\left.\begin{aligned} i\omega h S_-^*(\omega) + h\beta_+^*(\omega) &= -i\tilde{P}^*(\omega)\,\mathrm{sh}\,\omega(b-c) + i\omega\tilde{A}^*(\omega)\,\mathrm{ch}\,\omega(b-c), \\ -i\omega h T_-^*(\omega) + h\beta_+^*(\omega) &= iP^*(\omega)\,\mathrm{sh}\,\omega c - i\omega A^*(\omega)\,\mathrm{ch}\,\omega c. \end{aligned}\right\} \quad (3.14)$$

Here the subscripts $\pm$ signify functions of ω that are regular in the upper and lower half-planes respectively, and $h\beta(x)$ is the unknown transverse velocity at $y = c$ in $x < 0$. Also, if we define $h\gamma(x) = \partial V_2/\partial y(x, c-0) - \partial V_2/\partial y(x, c+0)$, then

$$h\gamma_-^*(\omega) = i\omega^2\tilde{A}^*(\omega)\,\mathrm{sh}\,\omega(b-c) - i\omega\tilde{P}^*(\omega)\,\mathrm{ch}\,\omega(b-c) - i\omega^2 A^*(\omega)\,\mathrm{sh}\,\omega c + i\omega P^*(\omega)\,\mathrm{ch}\,\omega c. \quad (3.15)$$

In the general situation where the thickness factor h, the relative tube widths b and c and the position factor μ are $O(1)$, the two viscous wall layers represented by (2.6*a*, *b*) and its counterpart for $\bar{Z} = O(1)$, with $F = G = 0$, supply two nonlinear relations between the unknown pressures and displacements. So in principle with (3.14) and (3.15) we have sufficient equations to fix γ_-^* and β_+^*. The elucidation of the nonlinear behaviour requires recourse to a numerical approach. Since the boundary-layer equations are involved there is the prospect of separation being induced in one or both of the outer wall layers by the insertion of the dividing wall or body in the inviscid interior, even when this interior blockage is of very small thickness. If $h \ll 1$, however, the two wall interactions become comparatively weak and progress can be made analytically. Expansion of the two viscous solutions along the lines of §3.1 produces the two extra pressure–displacement relations (3.1) and (3.2) with $F = G = 0$, in which the overbars denote functions divided by h. Hence, using (3.14) and (3.15) we obtain

$$\frac{\gamma_-^*(\omega)}{\omega} = \frac{1 - i\mu^{-\frac{1}{3}}\left(\dfrac{0+i\omega}{\theta}\right)^{\frac{1}{3}}\mathrm{th}\,\omega c}{\mathrm{th}\,\omega c - i\mu^{-\frac{1}{3}}\left(\dfrac{0+i\omega}{\theta}\right)^{\frac{1}{3}}}(\beta_+^* - i\omega T_-^*) + \frac{1 - i\mu^{-\frac{1}{3}}\left(\dfrac{0+i\omega}{\theta}\right)^{\frac{1}{3}}\mathrm{th}\,\omega(b-c)}{\mathrm{th}\,\omega(b-c) - i\mu^{-\frac{1}{3}}\left(\dfrac{0+i\omega}{\theta}\right)^{\frac{1}{3}}}(\beta_+^* + i\omega S_-^*) \quad (3.16)$$

for the determination of the functions $\gamma_-^*(\omega)$ and $\beta_+^*(\omega)$ by means of the Wiener–Hopf factorization technique. Interest is centred now on some of the limiting forms of the solution.

Letting c and $b \to \infty$ and using superposition of solutions, we may deal with a finite body and retrieve the results of thin-wing theory (see, for example, Thwaites 1960; Mikhlin 1964). Again, for a finite blockage, the limits $c \to 0$ and $b \to \infty$ (in that order) give rise to a situation similar to that of Brown & Stewartson

(1970), who performed the necessary factorization of (3.16). For a bifurcating channel, on the other hand, the length scale l [see (1.1)] is so far arbitrary. To fix it in general we must ensure that either c or b remains finite. Hence the above double limit may be inappropriate as far as a global solution is concerned. With that proviso, meaningful results are still obtainable in some formal limiting cases and as in § 3.1. perhaps the most interesting occurs when μ is small, implying that the bifurcation starts just downstream of the adjustment stage. We may anticipate that here again the overriding effect downstream lasts a distance $x \sim \mu^{-5}$, whereas the upstream influence effectively starts where $|x| \sim \mu^{-\frac{5}{7}}$, and this difference in length scales requires some deliberation. The wake effect follows from writing $\omega = \mu^5\Omega_1$ in (3.16). This gives to first order

$$\frac{\gamma_-^*}{\mu^5\Omega_1} = K(\Omega_1)\beta_+^* + \frac{i\Omega_1 S_-^*(0)}{\Omega_1(b-c) - i\left(\frac{0+i\Omega_1}{\theta}\right)^{\frac{4}{3}}} - \frac{i\Omega_1 T_-^*(0)}{\Omega_1 c - i\left(\frac{0+i\Omega_1}{\theta}\right)^{\frac{4}{3}}}, \tag{3.17}$$

where
$$K(\Omega_1) = K_-(\Omega_1) = \frac{\mu^{-5}\left[b\Omega_1 - 2i\left(\frac{0+i\Omega_1}{\theta}\right)^{\frac{4}{3}}\right]}{\left[\Omega_1 c - i\left(\frac{0+i\Omega_1}{\theta}\right)^{\frac{4}{3}}\right]\left[\Omega_1(b-c) - i\left(\frac{0+i\Omega_1}{\theta}\right)^{\frac{4}{3}}\right]}.$$

Examination of $\gamma(x)$ for $X_1 \ll 1$ shows that $\beta_+^* \equiv 0$ and so, as expected, no upstream disturbances are generated on this scale. In particular (3.17) gives the pressure at the upper wall as

$$\bar{P} = -\frac{3^{\frac{1}{2}}\mu^5\theta^4}{2\pi} S_-^*(0)(b-c)^2 \int_0^\infty \frac{\exp\left[-\xi X_1\theta^4(b-c)^3\right]}{1+\xi^{\frac{1}{3}}+\xi^{\frac{2}{3}}} \xi^{\frac{1}{3}} d\xi \tag{3.18}$$

for $X_1 > 0$ (and $\bar{P} \equiv 0$ for $X_1 < 0$). To uncover the major upstream response, which occurs on the $\mu^{-\frac{5}{7}}$ length scale, for convenience we set $c = \frac{1}{2}b \sim 1$ and consider a bifurcating wall that is wedge-like at its tip. Specifically we suppose that $(S-T)(x) = \hat{C}x\exp(-Cx)$, where $\mu^{-2n}\hat{C}$ and $\mu^{-n}C$ are order-one constants and $\frac{5}{7} < n < \frac{20}{7}$, so that (3.18) still holds since the effective length of the blockage is $o(\mu^{-5}l)$. With $|\omega| \ll 1$, (3.16) can be rewritten as

$$\gamma_-^*(\omega)/\omega K_-(\omega) - i\omega(S-T)_-^*(\omega + i\kappa\mu^{\frac{5}{7}}) = \beta_+^*(\omega)/K_+(\omega), \tag{3.19}$$

where
$$K(\omega) = \frac{K_-(\omega)}{K_+(\omega)} = \left[\frac{2 - i\mu^{-\frac{5}{3}}\left(\frac{0+i\omega}{\theta}\right)^{\frac{4}{3}} b\omega}{b\omega - 2i\mu^{-\frac{5}{3}}\left(\frac{0+i\omega}{\theta}\right)^{\frac{4}{3}}}\right], \tag{3.20a}$$

$$K_+(\omega) = (\omega + i\kappa\mu^{\frac{5}{7}})^{-1}. \tag{3.20b}$$

We extend the region of regularity of the + functions here to $\operatorname{Im}\omega > -i\kappa\mu^{\frac{5}{7}}$, which may be justified *a posteriori*. So both sides of (3.19) are entire in the strip $0 > \operatorname{Im}\omega > -i\kappa\mu^{\frac{5}{7}}$. The order of the singularity at the origin ($x = 0+$) is minimized if the left-hand side is also required to be bounded as $|\omega| \to \infty$, to avoid a catastrophic rise in the velocity near the blockage by ensuring that $\gamma(x)$ is integrable at $x = 0+$. Hence by analytic continuation both sides of (3.19) are

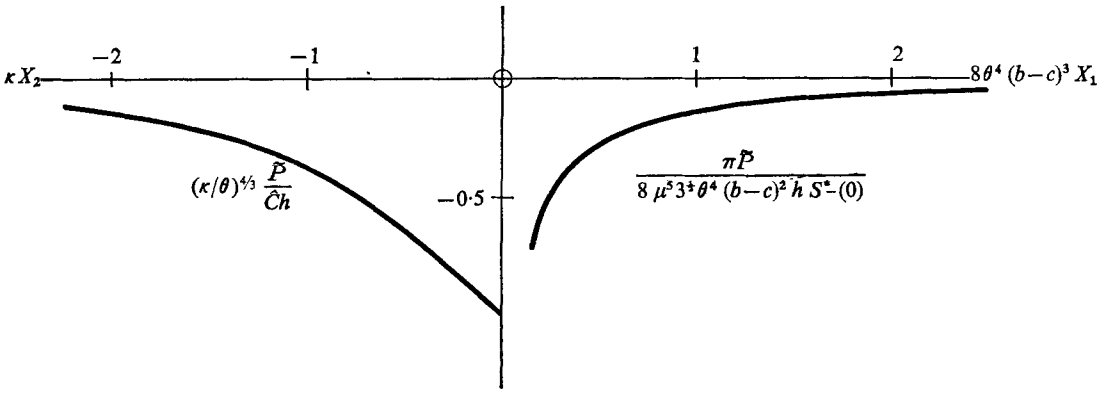

FIGURE 2. The long-scale upstream and wake pressure distribution $\bar{P}$ induced at the upper wall by a bifurcation of the channel for $\mu \ll 1$ when h is small.

equal to a constant, $\hat{D}$ say, and moreover $\hat{D} = i\hat{C}$. Upon inversion (3.19) now gives

$$\gamma(x) = -\frac{3^{\frac{1}{2}}\mu^{-\frac{5}{8}}\theta^{-\frac{1}{8}}}{2\pi}\int_0^\infty e^{-tx}\frac{[\hat{C}/(t-C)^2 + \hat{D}i/t(t+\kappa\mu^{\frac{5}{7}})]\,t^{\frac{1}{8}}(4+b^2t^2)\,dt}{b^2 + 2b\mu^{-\frac{5}{8}}\theta^{-\frac{1}{8}}t^{\frac{1}{8}} + 4\mu^{-\frac{1}{4}}\theta^{-\frac{5}{8}}t^{\frac{2}{8}}} \tag{3.21}$$

(the integral to be interpreted as a principal value), which is integrable at $x = 0$ since $\hat{D} = i\hat{C}$. Equation (3.21) may be used to give the upper-wall pressure, and for $x > 0$ and $O(\mu^{-5})$, the result agrees with (3.18). For $x < 0$ and $O(\mu^{-\frac{5}{7}})$ we have in addition

$$\bar{P}(X_2) = -\hat{C}(\theta/\kappa)^{\frac{1}{8}}\exp(\kappa\mu^{\frac{5}{7}}x), \tag{3.22}$$

to first order in μ. Hence if, say, the interior wall is thicker on its upper side, so that $S(x) \geqslant T(x) \geqslant 0$, then the pressure gradient driving the flow in the viscous wall layer far upstream of the branching is favourable. Far downstream it becomes adverse, however. The long-scale pressure gradient is drawn in figure 2.

A symmetric bifurcation, with $c = \frac{1}{2}b$ and $S(x) = T(x)$, is easier to analyse since $\beta(x)$ and $\gamma(x)$ are identically zero. The pressure transform is

$$\bar{P}^*(\omega) = -i\omega T^*(\omega)\Big/\left[i\,\mathrm{sh}\left(\frac{b\omega}{2}\right) + \left(\frac{0+i\omega}{\theta}\right)^{\frac{1}{8}}\mu^{-\frac{5}{8}}\,\mathrm{ch}\left(\frac{b\omega}{2}\right)\right]. \tag{3.23}$$

The limits $b \to 0$, $\mu \to 0$ and $\mu \to \infty$ are then quite straightforward, with little upstream influence generated owing to the symmetry. The limit $b \to \infty$, on the other hand, yields exactly the same result for the pressure as if the blockage ($T(x)$) of the flow were placed at the wall. So Smith's (1973) work becomes directly applicable, suggesting (see his figure 3) that the two boundary layers expand upstream under the adverse induced pressure gradient.

4. The adjustment in pipe flows

The underlying arguments governing the changeover stage may be modified to undeveloped symmetric or asymmetric flow through a semi-infinite pipe. The pipe is supposed to be straight and circular ahead of the constriction or blockage.

During the constriction or blockage, the flow for finite values of x becomes three-tiered, comprising an unknown inviscid potential core and a double-structured boundary layer adjoining the pipe wall $r = b$. Here $(l\bar{x}, lr, \phi)$ are cylindrical polar co-ordinates, and the relevant orders of magnitude are again found to be (1.2). The notation is essentially the same as for the two-dimensional flow except that bl is now the radius of the pipe and U_0 (v, w) are the radial and azimuthal fluid velocities respectively.

In the main part of the boundary layer, then, the solution in the adjustment stage is written as

$$\left.\begin{aligned} u &= U_B(Y) + \epsilon[u_1(x, Y, \phi) + U_{B1}(Y)], \quad v = -\epsilon^2 v_1(x, Y, \phi), \\ w &= \epsilon^2 w_1(x, Y, \phi), \quad p = \epsilon p_{1B} + \epsilon^2[p_1(x, Y, \phi) + p_{2B}] \end{aligned}\right\} \tag{4.1}$$

for Y of order unity, x denoting axial distance, effectively as in §2, and $r = b - \epsilon Y$. Also, $U_{B1}(Y)$ and the constants p_{1B} and p_{2B} are the corrections to the oncoming boundary-layer flow described by an axisymmetric analogue of (2.3) and (2.4). The Navier–Stokes equations simplify under (4.1) to give the solutions

$$\left.\begin{aligned} &p_1 = p_1(x, \phi), \quad w_1 = D(x, \phi)/U_B(Y), \quad \text{where} \quad \frac{\partial D}{\partial x} = -\frac{1}{b}\frac{\partial p_1}{\partial \phi}, \\ &v_1 = (-\partial A/\partial x)\, U_B(Y), \quad u_1 = A(x, \phi)\, U_B'(Y) \end{aligned}\right\} \tag{4.2}$$

from the r, ϕ and $\bar{x}$ momentum equations and the continuity equation respectively. Here the functions D, A and p_1 are independent of Y and are to be determined, but $D(-\infty, \phi) = 0$ since far upstream of the constriction or blockage the flow is axisymmetric. The order of magnitude of w in (4.1) stems from the requirement that the solution here should match with the thinner slip layer near the wall and with the inviscid core. Hence the secondary flow (v, w) generally has a two-dimensional character in this main deck, while the continuity equation is essentially a balance between the streamwise and radial mass flows only. It is anticipated that the unknown function $D(x, \phi)$, as well as $A(x, \phi)$ and $p_1(x, \phi)$, will be non-zero during the constriction or blockage. Consequently, when the wall is approached, not only does the streamwise displacement become comparable with the oncoming Blasius velocity, as in planar flow (§2), but also the swirl velocity w is singular.

In the $O(\epsilon^2)$ viscous sublayer, therefore, defined by $r = b - \epsilon^2 Z$ with $Z \sim 1$, the solution is expected to be of the form

$$\left.\begin{aligned} u = \epsilon U(x, Z, \phi), \quad v = -\epsilon^3 V(x, Z, \phi), \quad w = b\epsilon W(x, Z, \phi), \\ p = \epsilon p_{1B} + \epsilon^2 [P(x, Z, \phi)\, b^2 + p_{2B}]. \end{aligned}\right\} \tag{4.3}$$

The scaling for w in (4.3) is chosen to provide a significant contribution to the mass-flow balance and hence to the inertial forces, a requirement sufficient to fix the order of magnitude in (4.1). Consequently the secondary flow is effectively a one-dimensional motion, in the azimuthal direction only, near the wall and is jet-like since the swirl w is much greater here than in the main part of the boundary

layer. Substituting in the Navier–Stokes equations we obtain to first order in ϵ the three-dimensional boundary-layer equations

$$\left.\begin{aligned} \frac{\partial U}{\partial x}+\frac{\partial V}{\partial Z}+\frac{\partial W}{\partial \phi} &= 0, \\ U\frac{\partial U}{\partial x}+V\frac{\partial U}{\partial Z}+W\frac{\partial U}{\partial \phi} &= -\frac{\partial P}{\partial x}b^2+\frac{\partial^2 U}{\partial Z^2}, \\ U\frac{\partial W}{\partial x}+V\frac{\partial W}{\partial Z}+W\frac{\partial W}{\partial \phi} &= -\frac{\partial P}{\partial \phi}+\frac{\partial^2 W}{\partial Z^2}. \end{aligned}\right\} \tag{4.4a}$$

Here
$$P = P(x,\phi) = p_1(x,\phi)/b^2 \tag{4.4b}$$

from the radial momentum equation. The boundary conditions for (4.4a, b) are those of no slip at the wall, which is supposed to have the asymmetric shape $r = b-\epsilon^2 hF(x,\phi)$, with $h \sim 1$, and of matching with the oncoming axisymmetric boundary layer upstream and with the main deck away from the wall. Thus

$$U = V = W = 0 \quad \text{at} \quad Z = hF(x,\phi), \tag{4.4c}$$

$$U \sim \mu Z, \quad V \to 0, \quad W \to 0 \quad \text{as} \quad x \to -\infty, \tag{4.4d}$$

$$U \sim \mu(Z+A(x,\phi)), \quad V \sim -\mu Z\frac{\partial A}{\partial x}, \quad W \sim \frac{D(x,\phi)}{b\mu Z} \quad \text{as} \quad Z \to \infty. \tag{4.4e}$$

The third distinct flow region is the inviscid core, $0 \leqslant r < b$, in which

$$u = 1+\epsilon\hat{U}_1(r,\epsilon)+\epsilon^2 U_2, \quad (v,w) = \epsilon^2(V_2,U_2), \quad p = \epsilon p_{1B}+\epsilon^2(P_2+p_{2B}),$$

since v and w remain finite on entering the core from the main boundary layer. Here $\hat{U}_1(r,\epsilon)$, p_{1B} and p_{2B} again represent contributions from the boundary-layer displacement ahead of the adjustment zone, analogous to (2.7). The motion in the core is virtually a potential one again and we have to leading order

$$\partial(U_2,V_2,W_2)/\partial x = -\nabla p.$$

Then, from conservation of mass, the pressure perturbation $P_2(x,r,\phi)$ satisfies Laplace's equation

$$(\partial^2/\partial r^2+r^{-1}\partial/\partial r+r^{-2}\partial^2/\partial\phi^2+\partial^2/\partial x^2)P_2 = 0. \tag{4.5a}$$

The boundary conditions on P_2 here require that the pressure should be continuous with its value in the double boundary layer at the edge of the core, and that the radial influx $-V_2$ there should be given by the main-deck value of v_1 of (4.2) for $Y \to \infty$. Hence

$$P_2 = b^2 P(x,\phi), \quad \partial P_2/\partial r = -\partial^2 A(x,\phi)/\partial x^2 \quad \text{at} \quad r = b, \tag{4.5b}$$

from (4.4b) and (4.2). Continuity of the azimuthal velocity from the core to the main boundary layer is then assured. Further, if no rigid body is present on the pipe axis a condition of finite pressure must be imposed at $r = 0$. But when a thin symmetric blockage is sited along the axis the inviscid flow constraint of tangential flow there requires

$$\frac{\partial P_2}{\partial r} \sim -\frac{1}{r}\frac{d}{dx}\{xS'(x)\} \quad \text{as} \quad r \to 0 \tag{4.5c}$$

if the surface of the blockage is prescribed by $r = \epsilon S(x)$. During the following analysis we shall assume the absence of such blockage, however.

For h of order one, (4.2), (4.4) and (4.5) describe the nonlinear flow through the constricted pipe and necessitate a numerical treatment. Linearized solutions are valid if we now take $h \ll 1$, however. Then the flows in the viscous sublayer and inviscid core are expressible in the form $U = \mu Z + h\bar{U}, (V, W, P, A, D, P_2) = h(\bar{V}, \bar{W}, \bar{P}, \bar{A}, \bar{D}, \bar{P}_2)$ with corrections of order h^2. Substituting into the governing equations (4.4a) and neglecting terms $O(h^2)$, we have then the linear equations

$$\frac{\partial \bar{U}}{\partial x} + \frac{\partial \bar{V}}{\partial Z} + \frac{\partial \bar{W}}{\partial \phi} = 0, \tag{4.6a}$$

$$\mu Z \frac{\partial \bar{U}}{\partial x} + \mu \bar{V} = -\left(\frac{\partial \bar{P}}{\partial x}\right) b^2 + \frac{\partial^2 \bar{U}}{\partial Z^2}, \tag{4.6b}$$

$$\mu Z \frac{\partial \bar{W}}{\partial x} = -\frac{\partial \bar{P}}{\partial \phi} + \frac{\partial^2 \bar{W}}{\partial Z^2}. \tag{4.6c}$$

The boundary conditions become, under the same linearization procedure,

$$\bar{U} = -\mu F(x, \phi), \quad \bar{V} = \bar{W} = 0 \quad \text{at} \quad Z = 0, \tag{4.7a}$$

$$\bar{U} \to \mu \bar{A}(x, \phi), \quad \bar{V} \sim -\mu Z \, \partial \bar{A}/\partial z, \quad \bar{W} \sim \bar{D}/b\mu Z \quad \text{as} \quad Z \to \infty, \tag{4.7b}$$

$$\bar{U}, \bar{V}, \bar{W} \to 0 \quad \text{as} \quad x \to -\infty. \tag{4.7c}$$

When the Fourier transform (2.9) is applied, (4.6c) may first be solved for $\bar{W}^*$ in terms of the unknown function $\bar{D}^*(\omega, \phi)$, yielding

$$\bar{W}^* = -\mu^{-\frac{2}{3}}(0 + i\omega)^{\frac{1}{3}} \bar{D}^*(\omega, \phi) \, \mathscr{L}(t) \, b^{-1}, \tag{4.8}$$

where $$\mathscr{L}(t) = -\tfrac{2}{3} \times 3^{\frac{1}{2}} \int_0^\infty \sin\left(\tfrac{1}{3}\xi^3 + \xi t - \tfrac{1}{6}\pi\right) d\xi, \quad t = [\mu(0 + i\omega)]^{\frac{1}{3}} Z$$

and the wall condition on $\bar{W}$ is satisfied. This solution is then substituted into the Z derivative of the x momentum equation (4.6b), with (4.6a) serving to eliminate $\bar{V}$. Upon integration we have

$$\frac{\partial \bar{U}^*}{\partial t} = \hat{B}(\omega, \phi) \, \mathrm{Ai}\,(t) + \mu^{-\frac{2}{3}}(0 + i\omega)^{-\frac{2}{3}} \frac{\partial \bar{D}^*}{\partial \phi} \mathscr{M}(t) \, b^{-1}, \tag{4.9}$$

where $$\mathscr{M}(t) = \mathscr{L}'(t) + \mathrm{Ai}\,(t)/3\,\mathrm{Ai}^2\,(0).$$

The function $\hat{B}(\omega, \phi)$ is determined in terms of the unknowns $\bar{P}^*$ and $\bar{D}^*$ by setting $Z = 0$ in (4.6b):

$$\hat{B}(\omega, \phi)\,\mathrm{Ai}'\,(0)\,[\mu(0 + i\omega)]^{\frac{2}{3}} = i\omega b^2 \bar{P}^*(\omega, \phi) + \frac{\partial \bar{D}^*/\partial \phi}{\mathrm{Ai}(0)\, b} \int_0^\infty \mathrm{Ai}(\xi) \, \mathscr{L}(\xi) \, d\xi. \tag{4.10}$$

Integration of (4.9) with respect to Z from 0 to ∞ and use of the wall condition (4.7a) now yields the relation

$$\tfrac{1}{3}\hat{B}(\omega, \phi) + \frac{\partial \bar{D}^*/\partial \phi}{(\mu(0 + i\omega))^{\frac{2}{3}} b} \int_0^\infty \mathscr{M}(\xi) \, d\xi = \mu[\bar{A}^*(\omega, \phi) + F^*(\omega, \phi)], \tag{4.11}$$

where
$$i\omega\bar{D}^* = -b\,\partial\bar{P}^*/\partial\phi \tag{4.12}$$

from (4.2). The final requirement fixing, with (4.10)–(4.12), the solution for $\bar{A}^*$, $\bar{P}^*$, $\bar{D}^*$ and $\hat{B}$ comes from the potential core flow. To proceed further we assume that the indentation shape $F(x,\phi)$ is expressible as a Fourier cosine series. So we need only consider the case where F has the single component

$$F(x,\phi) = G(x)\cos m\phi,$$

$G(x)$ is a given function of x and m is a non-negative integer. The linearized flow may now be Fourier analysed, according to

$$\left.\begin{aligned} \bar{P}(x,\phi) &= \bar{p}(x)\cos m\phi, \quad \bar{D}(x,\phi) = \bar{d}(x)\sin m\phi, \\ \bar{A}(x,\phi) &= \bar{a}(x)\cos m\phi, \quad \bar{P}_2(x,r,\theta) = \bar{p}_2(x,r)\cos m\phi, \end{aligned}\right\} \tag{4.13}$$

and, combining (4.10)–(4.12), we obtain on equating coefficients of $\cos m\phi$

$$-\bar{p}^*(\omega)\,[(0+i\omega)^{\frac{1}{3}}\theta^{-\frac{4}{3}}b^2 - m^2 D_1/(0+i\omega)^{\frac{4}{3}}] = \mu^{\frac{4}{3}}[\bar{a}^*(\omega) + G^*(\omega)]. \tag{4.14}$$

Here the constants

$$D_1 = \int_0^\infty \mathscr{M}(\xi)\,d\xi + 2\pi C_1/3^{\frac{1}{2}} = 1{\cdot}289\ldots, \quad C_1 = -\int_0^\infty \mathrm{Ai}(\xi)\,\mathscr{L}(\xi)\,d\xi = 0{\cdot}112\ldots.$$

The transform of the core equation (4.5a) now gives the following solution for flow without an interior blockage: $\bar{p}_2^* = b^2\bar{p}^*(\omega)\,I_m(\omega r)/I_m(\omega b)$, where $I_m(z)$ is the modified Bessel function of the first kind and mth order. The ω-dependent coefficient is determined from the boundary condition on pressure at $r = b$. The radial pressure gradient at $r = b$ then relates $\bar{p}^*$ to $\bar{a}^*$ via the boundary condition (4.5b), which implies

$$\bar{a}^*(\omega) = \frac{I_m'(\omega b)\,b^2}{\omega I_m(\omega b)}\,\bar{p}^*(\omega). \tag{4.15}$$

Thus, in conclusion, (4.14) and (4.15) determine the solution for $\bar{a}^*(\omega)$ and $\bar{p}^*(\omega)$, while $\bar{d}^*(\omega)$ follows from $\bar{d}^* = bm\bar{p}^*/i\omega$.

The inversion of (4.14) and (4.15) is complicated in the general case, and it is more illuminating to study the various effects of the relative pipe radius b and the positioning factor μ. Two relatively simple results present themselves immediately. First, the general axisymmetric case $m = 0$ gives

$$\bar{P}^*(\omega) = \frac{-G^*(\omega)\,b^{-2}}{[(0+i\omega)^{\frac{1}{3}}/\mu^{\frac{4}{3}}\theta^{\frac{4}{3}} + I_0'(\omega b)/\omega I_0(wb)]}, \quad \bar{A}^*(\omega) = \frac{I_0'(\omega b)\,b^2\bar{P}^*}{\omega I_0(\omega b)} \tag{4.16}$$

and so for $b \gg 1$ we retrieve the external thin-wing (and quasi-two-dimensional) law between the pressure and streamwise displacement as in (3.4). Thus there is a merging with Smith's (1973) work on planar external flow. When $b \ll 1$ an analysis similar to that in (4.17)–(4.21) below shows a wake effect persisting over a large distance ($x \sim b^{-3}$) but only a small upstream response (for $x \sim b$). Second, if $\mu \gg 1$ the inviscid form, with the displacement fixed as $\bar{a} = -G$ and the pressure governed by straightforward linear inviscid theory, follows in a similar vein to § 3, provided x is not small. Here, with the indentation upstream of the adjustment zone, the boundary layer is still sufficiently thin and 'attached'

to the wall that viscous forces are insignificant and the major effects are those of a disturbance placed in a uniform stream. Very near the indentation, however (when $x \sim \mu^{-\frac{5}{4}}$), the work leading to (4.22)–(4.24) below becomes relevant. We now move on to consider the flow properties (i) when μ or b is small and (ii) when b is large, for an asymmetric disturbance.

(i) *If μ is small* then, in contrast to the channel flow situations beyond adjustment (§3), large-scale upstream influence is virtually non-existent, for any far solution is then dominated by the term in D_1 in (4.14), which initiates only a large wake effect as we now show. When $X_1 = \mu^5 x$ is of order unity (4.14) and (4.15) give

$$\bar{p}^* = \frac{\mu^{10} G^*(0)\,(0+i\Omega_1)^{\frac{2}{3}}}{D_1 m^2/i\Omega_1 - (0+i\Omega_1)^{\frac{2}{3}} bm/\Omega_1^2}$$

and so $$\bar{p}(x) = \frac{3^{\frac{1}{2}} G^*(0)\,\mu^{15} b^8}{2\pi D_1^9 m^{10}} \mathscr{J}_7(X_1), \quad \text{where} \quad \mathscr{J}_n(X_1) = \mathscr{H}_n\left(\frac{8X_1}{m^3}\right), \tag{4.17}$$

for $X_1 > 0$. But $\bar{p} = 0$ for $X_1 < 0$, and indeed no mechanism for substantial upstream propagation seems evident. Rather, because of the enhanced influence of the containing walls the upstream response when μ is small is confined to the neighbourhood of the constriction, where $|\omega|$ is $O(1)$ and (4.14) becomes

$$\bar{p}^*(\omega) = \frac{\mu G^*(\omega)\,(0+\mu i\omega)^{\frac{2}{3}}}{D_1 m^2/i\omega - b^2 i\omega/\theta^{\frac{4}{3}}}.$$

Taking the example of a point disturbance for convenience, we then have that for x positive and finite

$$\bar{p}(x) = \mu^{\frac{5}{3}} G^*(0)\,\lambda^{\frac{2}{3}} \frac{\theta^{\frac{4}{3}}}{b^2}\left[\tfrac{1}{4} e^{-\lambda x} - \frac{3^{\frac{1}{2}}}{2\pi}\int_0^\infty \left(\frac{e^{-\lambda\xi x}\xi^{\frac{5}{3}} - e^{-\lambda x}}{\xi^2 - 1}\right) d\xi\right] \tag{4.18}$$

since poles exist in the upper and lower half-planes at $\omega = \mp i\lambda$, where $\lambda = D^{\frac{1}{3}} m \theta^{\frac{2}{3}} b^{-1} = mb^{-1}$. When x is $O(1)$ and negative the pole in $\operatorname{Im}\omega < 0$ gives

$$\bar{p}(x) = \tfrac{1}{2}\mu^{\frac{5}{3}} G^*(0)\,\lambda^{\frac{2}{3}}\theta^{\frac{4}{3}}/b^2\, e^{\lambda x}. \tag{4.19}$$

Hence downstream the local solution (4.18) merges with the far-wake solution (4.17) as $X_1 \to 0+$, and there are two main scales for this flow (figure 3). One is close to the indentation, where the pressure rises upstream [in (4.19)], also rises immediately downstream [in (4.18)] but eventually decreases. The other scale describes the far wake, where the pressure continues to drop [in (4.17)] but the motion changes its basic character. For, whereas the local flow is controlled by the axial and azimuthal pressure forces, with the displacement of little importance, in the far wake the displacement of the core due to the boundary layer dictates the flow features along with the azimuthal pressure gradient. We find also that in the far wake

$$(\tau - \mu, \tau_\phi, D, A'(x)) = \frac{hG^*(0)\,\mu^8 b^4}{2\pi \times 3^{\frac{1}{2}} m^8 D_1^8}\Big(-9C_1 m^4 D_1^4[\mathscr{J}_2 + \mathscr{J}_3]\cos m\phi,$$

$$\times \mu^5 b^3[\mathscr{J}_5 + \mathscr{J}_6]\sin m\phi/\mathrm{Ai}(0), -3(\mu b D_1 m)^2 \mathscr{J}_4 \sin m\phi, 3(\mu b D_1 m)^2 \mathscr{J}_4 \cos m\phi)\Big) \tag{4.20}$$

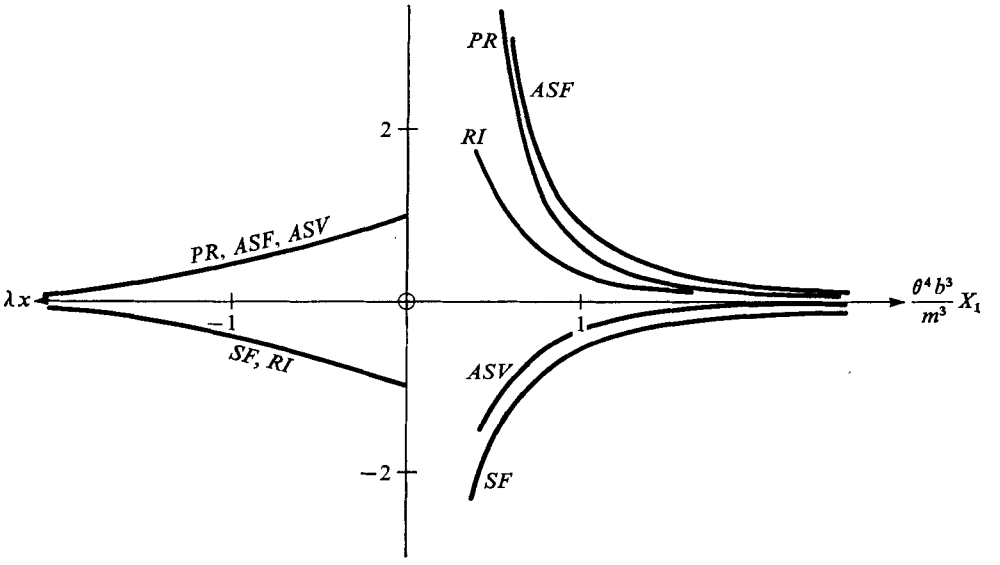

FIGURE 3. Linearized solutions, when $\mu \ll 1$, for the predominant three-dimensional flow upstream and downstream of an asymmetric constriction [see above (4.13)] in a pipe. Here *PR*, *SF*, *ASF*, *ASV* and *RI* stand for the scaled pressure, axial skin-friction perturbation, azimuthal skin friction, azimuthal slip velocity and radial inflow, given by

$$2\bar{p}b^2/\mu^{\frac{5}{3}}\theta^{\frac{4}{3}}\lambda^{\frac{8}{3}}G^*(0), \quad 2\lambda^{\frac{8}{3}}(\tau-\mu)\,b^2/3hm^2\mu^{\frac{4}{3}}G^*(0)\,\{\mathrm{Ai}\,(0)-C_1\}\cos m\phi,$$

$$6\,\mathrm{Ai}\,(0)\,\tau_\phi b^2/hm\mu^{\frac{4}{3}}\lambda^{\frac{1}{3}}\theta^{\frac{4}{3}}G^*(0)\sin m\phi, \quad 2\lambda^{\frac{1}{3}}b\bar{d}/m\mu^{\frac{5}{3}}\theta^{\frac{1}{3}}G^*(0) \quad \text{and} \quad 2b\lambda^{\frac{1}{3}}\bar{a}'(x)/m\mu^{\frac{5}{3}}\theta^{\frac{4}{3}}G^*(0)$$

respectively for $x < 0$. In $X_1 > 0$,

$$PR = 2\pi D_1^9 m^{10}b^{-8}\bar{p}/3^{\frac{1}{2}}\mu^{15}G^*(0), \quad SF = 2\pi b^{-4}m^4D_1^4C_1^{-1}(\tau-\mu)/3^{\frac{3}{2}}\mu^8G^*(0)\,h\cos m\phi,$$

$$ASF = 2\pi 3^{\frac{1}{2}}\,\mathrm{Ai}\,(0)b^{-7}m^8D_1^8\tau_\phi/\mu^{13}G^*(0)h\sin m\phi, \quad ASV = 2\pi b^{-6}m^6D_1^6\bar{d}/3^{\frac{1}{2}}\mu^{10}G^*(0)$$

and

$$RI = 2\pi(b^{-1}mD_1)^6\,\bar{a}'(x)/3^{\frac{1}{2}}\mu^{10}G^*(0).$$

for X_1 of order one and positive. Here τ_ϕ is the effective azimuthal shear stress $(\partial W/\partial Z)_{Z=0}$. In $x < 0$, on the other hand,

$$(\tau-\mu, \tau_\phi, D, A'(x)) = \frac{hG^*(0)\,\mu^{\frac{4}{3}}m\theta^{\frac{4}{3}}}{2\lambda^{\frac{1}{3}}b^2}\left(-\frac{2{\cdot}643m}{\lambda^{\frac{1}{3}}}\,\mathrm{Ai}\,(0)\cos m\phi, \frac{\lambda^{\frac{8}{3}}}{3\,\mathrm{Ai}\,(0)}\sin m\phi,\right.$$

$$\left.\mu^{\frac{1}{3}}b\sin m\phi, -\mu^{\frac{1}{3}}b\cos m\phi\right)e^{\lambda x} \quad (4.21)$$

when $|x|$ is finite. The solutions in these local upstream and far downstream zones are presented graphically in figure 3 and their physical interpretations appear to be as follows. Locally, ahead of the constriction the pressure in line with the constriction peak ($\phi = 0$) rises and produces the characteristic two-dimensional effect (cf. Smith 1973) of a fall in the streamwise skin friction τ, unaided by the increasing axial displacement $-A(x, 0)$ (see below). This causes the fluid just outside the viscous sublayer to be expelled outwards azimuthally ($D(x, 0) > 0$) as from a source. Fluid within the viscous sublayer jet is also driven away from the peak azimuthally by the adverse streamwise pressure gradient and the azimuthal outflow. Far downstream, however, the pressure in line with the peak is positive

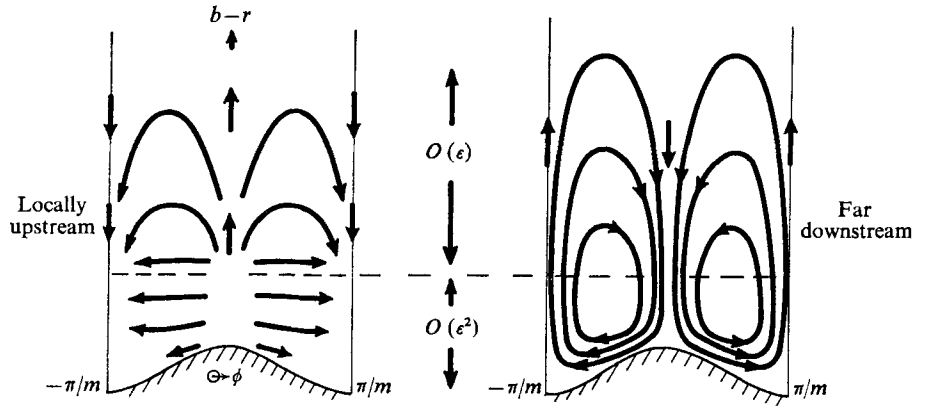

FIGURE 4. Sketch of the secondary pipe-flow response in the boundary layer immediately ahead of and far beyond the constriction $F = G\cos m\phi$ when $\mu \ll 1$.

but decreasing, so that the axial skin friction rises towards is value far upstream and induces an azimuthal inflow, towards the peak, at the edge of the sublayer. The azimuthal shear stress is positive near the constriction peak however and so there is outflow near the wall. Thus in the far wake the secondary flow throughout the two-tiered boundary layer, between two consecutive troughs of the indentation, consists of a pair of vortices symmetrically disposed on either side of the constriction peak but rotating in opposite senses. Figure 4 gives a sketch of the local upstream and far downstream secondary flow patterns.

The basic reasons for the initiation of the large-scale disturbances upstream in the above pipe flow are the balancing of the axial and azimuthal pressure gradients and the diminished influence of the core flow. Since the oncoming boundary layer is thicker and much less attached when μ is small, the fluid near the wall is affected more than that in the interior and so the core suffers practically no displacement. Accordingly, when the peak axial pressure gradient rises, inducing a fall in the peak axial shear stress τ, the fluid in the viscous sublayer must (in the absence of any core displacement) tend to swirl away from the peak. The azimuthal shear stress τ_ϕ therefore rises and the associated azimuthal pressure gradient must fall. The swirling then tends to enhance the increase in the axial shear in a trough and the whole process is reinforced. Conversely, far downstream the axial pressure gradient decays faster than the azimuthal gradient and when x is as large as $O(\mu^{-5})$ the dominant azimuthal pressure force itself becomes so weak that the minor core displacement at last plays a deciding role. This displacement is then linked to the pressure force by the parabolic law $\bar{p} = -\bar{a}''(x)/mb$, which is characteristic of a comparatively thin tube. (The law arises from the radial convection of momentum which is induced in the displaced core and with which the radial pressure gradient must balance.) Thus the positive pressure downstream produces a decreasing displacement ($\bar{a} > 0$) and there is entrainment of fluid into the viscous sublayer. However, the axial pressure gradient is negative, causing the peak axial shear stress τ to increase, and the overall movement of fluid radially towards the peak results in a swirl away from the peak near the wall. Hence the vortex-like nature of figure 4 is established.

If b is small a similar phenomenon appears. Upstream the characteristic length scale is that associated with the pipe width and so is small ($x = O(b)$) but downstream it is large ($x = O(b^{-3})$). The balancing of the pressure forces and the core displacement in each regime is then exactly as for the case $\mu \ll 1$.

(ii) The second form of interaction of most interest is due to the effects of relative enlargement of the pipe, when $b \gg 1$ and the core is virtually unaffected save close to the pipe walls. A three-dimensional extension of Stewartson's (1974) triple-deck theory holds here, the pressure–displacement law being that of linearized inviscid theory;

$$\bar{a}^*(\omega) = |\omega|\omega^{-2}\bar{p}^*(\omega)\, b^2, \tag{4.22}$$

to first order provided that $|x| \ll b$. The most persistent interactions in fact take place on a length scale comparable with the pipe's radius b, i.e. large relative to the indentation length, so that again there are two characteristic scales. We consider here only the features local to the indentation ($|x| \ll b$), which are of a character quite different from those where the pipe width and indentation length are comparable. These effects are governed by the properties of the transforms when ω is finite, in which case (4.14) becomes

$$\bar{p}^* = -\mu^{\frac{5}{3}} G^*(\omega)\, b^{-2} \Big/ \left[\frac{(0+i\omega)^{\frac{1}{3}}}{\theta^{\frac{4}{3}}} + \mu^{\frac{5}{3}} \frac{|\omega|}{\omega^2}\right]. \tag{4.23}$$

Despite the asymmetry the solutions for the pressure, axial skin friction τ and displacement $\bar{a}$ are effectively those given in Smith's (1973) planar flow study. Those for $\bar{d}$ and τ_ϕ are

$$(\pi b/m\mu^{\frac{1}{4}}\theta G^*(0))\,\bar{d} = \mathscr{J}(0,0,0)\,(x<0) \quad \text{or} \quad -\mathscr{J}(-\tfrac{1}{2}\times 3^{\frac{1}{2}},0,1) \quad (x>0), \tag{4.24}$$

$$\left(\frac{6\pi b^2\,\mathrm{Ai}\,(0)}{mh\theta^{\frac{5}{3}}\mu^{\frac{7}{4}}G^*(0)}\right)\frac{\tau_\phi}{\sin m\phi} = \mathscr{J}(0,2,0)\,(x<0) \quad \text{or} \quad \mathscr{J}(-3^{\frac{1}{2}},2,1) \quad (x>0),$$

where $$\mathscr{J}(\alpha,\beta,\gamma) = \int_0^\infty \exp\left(-\theta\xi|x|\,\mu^{\frac{5}{4}}\right)\frac{(1+\alpha\xi^{\frac{4}{3}})\,\xi^{\beta/3}}{(1-\gamma\times 3^{\frac{1}{2}}\xi^{\frac{4}{3}}+\xi^{\frac{8}{3}})}\,d\xi$$

and again we take $G(x)$ to be a point disturbance. Figure 5 gives the solution curves for the upstream and downstream flows here. In both the present limiting situation and that studied in (4.17)–(4.21), the role of the indentation as a point disturbance means that the solutions are singular just aft of the indentation (and possibly just upstream) when viewed on the predominant long length scale and that the flow properties local to the indentation are left to a smaller-scale analysis. We note that the inverse-square behaviour of the pressure in (4.23) as $|x| \to \infty$ is consistent with the dipole-like nature (see Smith 1973) of the quasi-external motion for $|x| \gg 1$, for there the flow suffers a simple displacement ($\bar{a} = -G$) and the pressure is specified by thin-wing theory.

In the present case of a comparatively wide tube the *far* wake (x large and positive) has properties that are qualitatively almost the same as those for a finite tube beyond the adjustment stage ($\mu \ll 1$, figures 3 and 4). Vortices rotating in the same sense as in figure 4 are again provoked throughout the two-tiered boundary layer. In the majority of the boundary layer fluid is drawn from the

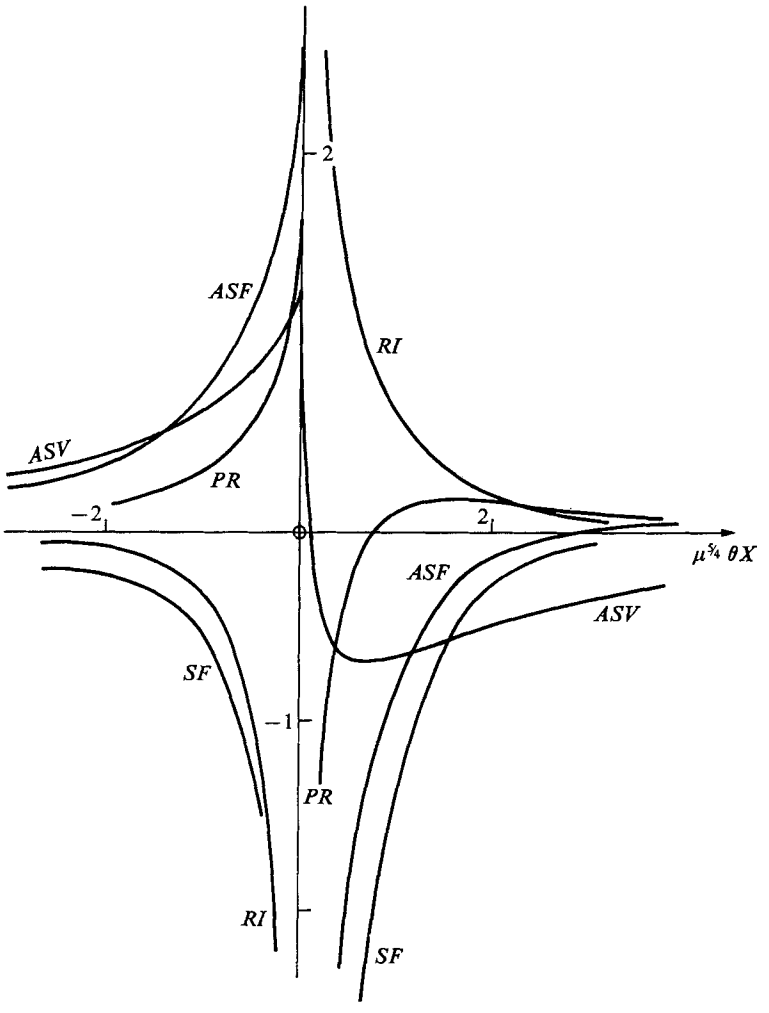

FIGURE 5. Graphs of the linearized pipe-flow interaction ahead of and beyond the asymmetric indentation $F = G\cos m\phi$ when $b \gg 1$. Here $PR = b\pi\mu^{-\frac{1}{2}}\theta^{-2}(G^*(0))^{-1}\bar{p}$,

$$SF = 2\pi\mu^{-3}\theta^{-\frac{1}{2}}(\tau-\mu)/3h\,\mathrm{Ai}\,(0)\,G^*(0)\cos m\phi,$$

$$ASF = 6b^2\pi\mu^{-\frac{7}{2}}\,\mathrm{Ai}\,(0)\,\theta^{-\frac{1}{2}}\tau_\phi/hmG^*(0)\sin m\phi,$$

$$ASV = b\pi\mu^{-\frac{1}{2}}\bar{d}/m\theta G^*(0) \quad \text{and} \quad RI = \pi\mu^{-\frac{1}{2}}\bar{a}'(x)/\theta^2 G^*(0).$$

core above a peak and expelled above a trough. The vortex motion here is again generated by the overall movement radially, towards the wall, of the fluid in line with the peak, since the boundary layer, having been displaced from the wall, must now retrieve the original Blasius form. The combined effect of the radial inflow and decreasing axial stress τ is therefore the azimuthal swirl, away from the peak, which produces the vortex behaviour. Although the pressure response is now different from that when μ is small, because its relation to the displacement is quasi-external, it plays little part in the final vortex structure. The displacement appears to be the dominant influence in the far wake. Likewise, upstream of the indentation the flow response is in some respects similar to that occurring when

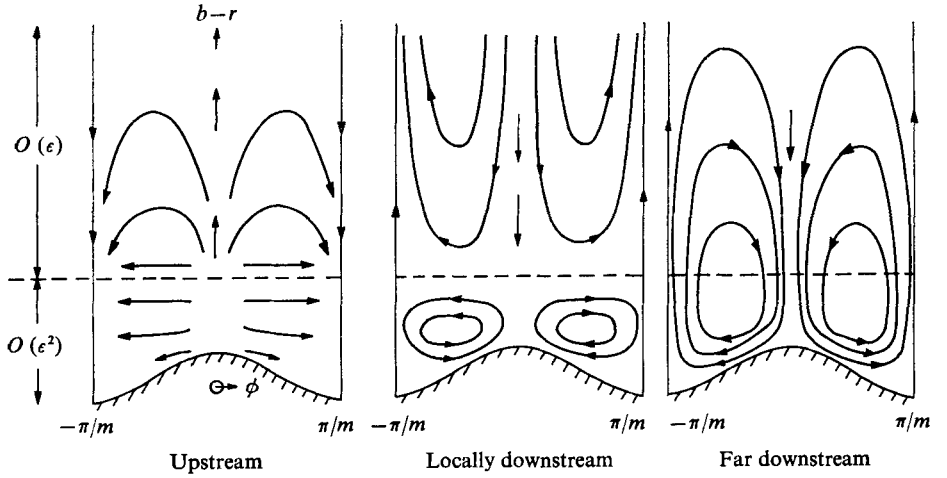

FIGURE 6. Sketch of the secondary flow induced in the boundary layer upstream and downstream of the asymmetric constriction $F = G\cos m\phi$ in a pipe if $b \gg 1$.

$\mu \ll 1$, but now the core displacement exerts a substantial influence. The presence of the indentation is anticipated throughout the boundary layer by a displacement radially from the wall along the peak line, accompanied by a rise in the pressure and a fall in the axial stress τ there. The associated displacement of the core then maintains the peak pressure rise and provokes the azimuthal slip velocity towards a trough. The outward swirl in the viscous layer produced by this slip is sustained by the relatively small azimuthal pressure gradient and so the source-like behaviour of the secondary flow upstream shown in figure 6 is encountered. Downstream, however, the azimuthal stress τ_ϕ and slip $\bar{d}$ do change sign, so that within the viscous sublayer the induced perturbations in the *near* wake of the constriction are almost totally the reverse of those in the far wake. The boundary-layer displacement must fall after the indentation and so there is inflow at the edge of the viscous layer. On the other hand, having encircled the obstacle the fluid has to move behind the obstacle, towards the peak line, and does so mostly in the slower flow region near the wall (where the axial skin friction τ has been diminished by the presence of the indentation and the boundary layer is less attached). The azimuthal concentration of fluid towards the peak then forces a radial movement away from the wall. That, combined with the radial inflow at the edge of the viscous layer, leads to an azimuthal slip away from the peak line. Hence a vortex is formed (figure 6), within the viscous layer alone, between a peak and a trough and rotates in the direction opposite to that of the vortex formed far downstream.

The above approach has also been used to investigate the properties of flow past an obstacle placed in the interior of the pipe, as in the planar case of §3.2. For the symmetric flow specified by (4.5*c*) we find that when μ is small, for example, there is a strong downstream influence on a length scale $O(l\mu^{-5})$ but very little upstream influence. An asymmetric blockage is more cumbersome to deal with but large upstream and/or wake effects of the types studied in (4.17)–(4.24) are most likely to be present.

5. Further discussion

It is felt that the linearized solutions derived above provide enough information to allow some confidence in the proposed structure of the motion in the primary adjustment stage, defined by (1.2). They also give qualitative insight into the influence that the entry flow can exert on a constricted or blocked tube flow, whether the constriction or blockage occurs quite near the inlet or far downstream. Certain of the aspects of this entry-flow influence in indented channels or pipes are not unexpected. For $b \gg 1$, for example, the direct link with the external flow features given by Smith (1973) was to be anticipated at the outset. However, even the properties of the motions when $b \ll 1$ are perhaps somewhat surprising. For despite the fact that the oncoming flow is not fully developed, since the leading-edge boundary layers have not yet merged, the relation between the pressure, the displacement of the core and the wall shape has already acquired the form characteristic of a fully developed initial velocity profile (Smith 1976*b*).

More intriguing is the nature of the constricted or bifurcating channel flow when an asymmetric disturbance is sited just downstream of the adjustment position, so that $\mu \ll 1$. The solution anticipates the interaction study by Smith (1977), in that the long-scale upstream and wake effects which are propagated are initiated by the transverse pressure gradient acting in the main body of the fluid. This pressure gradient forces movement of the fluid across the channel, an action which tends to accentuate the upstream growth or compression of the oncoming boundary layers and leads to a free interaction, both when the initial flow is fully developed (Smith 1977) and when it is only virtually so (§3 above).

Likewise, the more novel aspects of asymmetrically constricted pipe flows occur for $\mu \ll 1$, when the upstream influence is generated over a length scale comparable with the indentation length (rather than over the long length scale that occurs in planar flow). By contrast the downstream influence persists over a much greater distance. The gross effects that are induced are then wholly three-dimensional and viscous in origin. The flow properties depend crucially on the ratio b as well, of course, in so far as that ratio fixes the interplay between the induced pressure and the displacement at the edge of the core. When b is large the influence of an asymmetric indentation matters most in the vicinity of the wall, since the core remains almost undisturbed. Also, the azimuthal pressure gradient is of importance only in that it determines the secondary flow. Hence the pressure–displacement law is quasi-two-dimensional.

For a tube of finite relative width ($b = O(1)$) a constriction beyond adjustment ($\mu \ll 1$) induces an expansion of the boundary layer at a finite distance upstream, and, albeit much further downstream, vortex motion arises close to the wall. But when the tube is sufficiently enlarged ($b \gg 1$) the corresponding change in the pressure–displacement law is such that the same size of constriction instead induces a vortex flow rotating in the opposite direction just downstream, although a somewhat similar type of vortex motion is promoted far beyond the constriction. Thus the primary adjustment stage, occurring a large distance $O(R^{\frac{1}{3}}l)$ from the inlet (but before the oncoming boundary layers even start to coalesce) and

governing the initial switch from undeveloped to partially developed characteristics, would seem to specify one of the most vital areas for the siting of interior or wall disturbances.

In summary, then, the effect of the *position* $\bar{x}_0$ of the indentation is as follows (for an indentation of length comparable with the tube width, where $b = O(1)$). If the position is upstream of the adjustment stage (so that $\bar{x}_0 \ll 1$ and $\mu \gg 1$) the motion is effectively an inviscid perturbation of the uniform inlet stream. The boundary layers upstream are still so thin that they have little influence on the main flow properties. If the position is within the adjustment regime, however, the boundary layers do affect the motion and, when the indentation is moved still further downstream ($\bar{x}_0 \gg 1$ and $\mu \ll 1$), the boundary-layer influence becomes almost wholly dominant. For example, in pipe flow the induced motion is entirely viscous upstream when $\mu \ll 1$, and the core displacement is negligible, while in a channel the core simply suffers a transverse displacement. The effect of indentation *length* when the indentation is within the adjustment zone ($\mu = O(1)$) is governed by the ratio b. When the length is much greater than the tube width ($b \ll 1$) the influence of the inviscid core is correspondingly diminished and viscous effects dominate in similar fashion to the case $\mu \to 0$. If the indentation length is contracted ($b \gg 1$), however, the local motion, though remaining viscous, becomes quasi-external because in a channel, for instance, the walls are then relatively far apart. In a pipe the same quasi-external properties are recovered when $b \to \infty$, and a three-dimensional extension of triple-deck theory emerges.

Some work on extending the three-dimensional theory (§4) to fully developed pipe flows has now been done (Smith 1976*c*). The extra influence of unsteadiness in the flow can also be dealt with to some extent, by proceeding along the lines of the studies of Brown & Daniels (1975) and Smith (1976*b*).

The referees are thanked for pointing out some flaws in the original presentation and analysis.

REFERENCES

Brown, S. N. & Daniels, P. G. 1975 On the viscous flow about the trailing edge of a rapidly oscillating aerofoil. *J. Fluid Mech.* **67**, 743–761.

Brown, S. N. & Stewartson, K. 1970 Trailing-edge stall. *J. Fluid Mech.* **42**, 561–584.

Jones, D. S. 1952 A simplifying technique in the solution of a class of diffraction problems. *Quart. J. Math.* **3**, 189–196.

Mihklin, S. G. 1964 *Integral Equations*. Pergamon.

Noble, B. 1958 *The Wiener–Hopf Technique*. Pergamon.

Singh, M. P. 1974 Entry flow in a curved pipe. *J. Fluid Mech.* **65**, 517–539.

Smith, F. T. 1973 Laminar flow over a small hump on a flat plate. *J. Fluid Mech.* **57**, 803–824.

Smith, F. T. 1976*a* Fluid flow into a curved pipe. *Proc. Roy. Soc.* A **351**, 71–87.

Smith, F. T. 1976*b* Flow through constricted or dilated pipes and channels. *Quart. J. Mech. Appl. Math.* **29**, 343–364.

Smith, F. T. 1976*c* Pipeflows distorted by nonsymmetric indentation or branching. *Mathematika*, **23**, 62–83.

Smith, F. T. 1977 Upstream interactions in channel flows. *J. Fluid Mech.* (to appear).

STEWARTSON, K. 1974 Multistructured boundary layers on flat plates and related bodies. *Adv. in Appl. Mech.* **14**, 145–239.

STEWARTSON, K. & WILLIAMS, P. G. 1969 Self-induced separation. *Proc. Roy. Soc.* A **312**, 181–207.

THWAITES, B. (ed.) 1960 *Incompressible Aerodynamics*. Oxford University Press.

VAN DYKE, M. 1970 Entry flow in a channel. *J. Fluid Mech.* **44**, 813–823.

WILSON, S. D. R. 1971 Entry flow in a channel. Part 2. *J. Fluid Mech.* **46**, 787–799.